

# UNIVERSITY OF CINCINNATI

Date: \_\_\_\_\_

I, \_\_\_\_\_,  
hereby submit this work as part of the requirements for the degree of:

\_\_\_\_\_

in:

\_\_\_\_\_

It is entitled:

\_\_\_\_\_

\_\_\_\_\_

\_\_\_\_\_

\_\_\_\_\_

**This work and its defense approved by:**

**Chair:** \_\_\_\_\_

\_\_\_\_\_

\_\_\_\_\_

\_\_\_\_\_

\_\_\_\_\_

**Error Analysis of the Exponential Euler Method and the Mathematical  
Modeling of Retinal Waves in Neuroscience**

A dissertation submitted to the

Division of Research and Advanced Studies  
Of the University of Cincinnati

in partial fulfillment of the  
requirements for the degree of

**DOCTOR OF PHILOSOPHY (Ph.D)**

in the Department of Mathematical Sciences  
of the College of Arts and Sciences

June, 2005

by

**Jiyeon Oh**

B.S., Ewha Womans University, South Korea, 1999

Committee Chair: Dr. Donald A. French

## ABSTRACT

The exponential Euler method is a specialized numerical method that was used in a software package called GENESIS which was created to model neurons and neuronal networks. In this thesis we provide a convergence analysis for this scheme in the context of some standard models from neuroscience. We provide several computational examples to further study the accuracy. We also briefly consider a simple model of neuronal network activity waves.

There are two major parts to this dissertation. The first part concentrates on the error analysis of the exponential Euler scheme. The basic scheme is first order accurate. A second order modification is introduced. We also show how this exponential Euler method can be applied to mathematical models of neuronal networks that involve integro-differential equations. We prove a convergence theorem for this case.

The second part of this dissertation focuses on the modeling of retinal waves in the visual cortex. We propose a firing rate model for amacrine cells.

## ACKNOWLEDGEMENT

First of all, I would like to praise my Lord and Savior Jesus Christ who is always with me and provides me the best. Without Him, my life is worthless. I am also grateful to many others and would like to acknowledge their significant contributions to my study in the following:

- Professor Donald A. French, who has provided me constant supports and kind guidance. He is the best professor I have ever met in my life. My words are not enough to thank him.
- Professor Charles Groetsch and Bingyu Zhang, for being the committee members.
- Taft Foundation and NSF Grant for their financial support.
- Former and Current graduate students in the Mathematical Department.
- People at the Power Mission Baptist Church of Cincinnati especially Deacon Ahn's family and Pastor Lee's family.

Finally, I would like to express my deepest love to my husband, Kyesang Yoo, my son, Shiwon, my parents, parents-in-law, my sisters, and sisters(brothers)-in-law for their constant supports, love, encouragement and prayers.

# Contents

<b>1</b>	<b>Introduction</b>	<b>4</b>
1.1	Error Analysis of Exponential Euler Method . . . . .	5
1.2	Mathematical Modeling of Retinal Waves in Visual Cortex . . . . .	7
<b>2</b>	<b>Mathematical Neuroscience</b>	<b>10</b>
2.1	Neuron and Action Potential . . . . .	10
2.2	Morris-Lecar Model . . . . .	13
2.3	FitzHugh-Nagumo Equation . . . . .	16
2.4	Hodgkin-Huxley Model . . . . .	18
2.5	Integro-Differential Equations . . . . .	19
<b>3</b>	<b>Error Analysis of Exponential Euler Method</b>	<b>21</b>
3.1	Derivation and Motivation . . . . .	22
3.2	Error Estimation for the Basic Exponential Euler Scheme: . . . . .	23

3.3	Error Estimate for the Modified Exponential Euler Scheme . . . . .	30
3.4	Qualitative Analysis of the Scheme . . . . .	33
3.5	Application to an Integro-Differential Equation . . . . .	36
3.6	Applications to Partial Differential Equations . . . . .	45
3.7	Numerical Results . . . . .	47
<b>4</b>	<b>Mathematical Model of Retinal Waves in Visual Cortex</b>	<b>54</b>
4.1	Model Description . . . . .	56
4.2	Computational Results . . . . .	61
4.3	Integro-Differential Equation Modeling . . . . .	64
4.4	Future Work . . . . .	65

# Chapter 1

## Introduction

Mathematics has been frequently used to describe and understand the major processes of the nervous system. Mathematical neuroscience has two main goals. The first goal is to develop suitable mathematical models that describe the properties in the nervous system. The other important goal is to use these models to make predictions and understand how the nervous system works.

There are two major parts in this dissertation. The first part concentrates on the error analysis of the exponential Euler scheme that is a specialized numerical method for computing approximate solutions to the mathematical models in neuroscience. And the second part focuses on the modeling of retinal waves in the visual cortex.

## 1.1 Error Analysis of Exponential Euler Method

Mathematical models in neuroscience usually consist of systems of ordinary differential equations (ODEs). The basic equation for the electrical activity of a neuron was developed by Hodgkin and Huxley in their Nobel Prize winning work in the 1950's and consists of four ODEs ([HK] and [HH]). The FitzHugh-Nagumo equations form another model for a neuron's activity (See [KS] for an overview). These models can be solved by Runge-Kutta or Euler (forward or backward) methods as well as standard ODE solver packages. However, these schemes do not exploit the structure that exists in the neuron models.

Nonstandard methods are numerical schemes constructed to solve differential equations which have special properties (See [AL], [M1], [M2], [M3], or [RU]). In general, these schemes consist of special representations for nonlinear terms and more complex functional forms for the step sizes. The major advantages of nonstandard methods are that they often provide better approximations than those of conventional schemes in many situations. Although many such schemes have been introduced and studied computationally; except for [RG], there have been very few that offer a rigorous error analysis.

The exponential Euler method is a nonstandard method that was introduced by computational neuroscientists. It was used as a default integration method in

GENESIS which is a popular package for the simulation of neuronal systems [BB]. The scheme is explicit like forward Euler, but the data shows that it is stable for large time steps; however, in [BB], it is noted that it is difficult to rigorously analyze the error of the scheme (see page 334 of [BB]) and it is not as accurate as the forward Euler method with the same step size. In this dissertation we provide this rigorous error analysis. Our estimate shows that the exponential Euler method is first order accurate.

Most ODE discretization schemes (e.g. Runge Kutta, Multistep, etc) can be extended to provide higher-order accuracy. However, the exponential Euler scheme introduced in [BB] is only first order accurate. Using the Runge-Kutta technique for extrapolation, we provide a second order modification of the exponential Euler scheme.

A certain type of integro-differential equation has frequently been used to describe neuronal activity in a synaptically coupled neuronal network ([PE], [TEY]). We have applied the exponential Euler scheme to the integro-differential equation and have shown that this scheme is first order accurate.

When dendrite and axonal structures are included in neuron models, the resulting mathematical system typically involves time-dependent nonlinear partial differential equations (see [KS] for an overview). We briefly discuss methods based on splitting schemes combined with the exponential Euler method.

## 1.2 Mathematical Modeling of Retinal Waves in Visual Cortex

The second part of this dissertation focuses on the mathematical models of retinal waves in the visual cortex. Most neuronal systems are very complicated, and their mathematical models will have many parameters and variables. Often, simplified minimal models are sufficient to analyze and interpret the neuronal system.

Synchronized bursting activity generated by synaptically connected networks can be detected by multielectrode recordings and fluorescence imaging of calcium indicators can detect modulations in the levels of cytoplasmic calcium throughout the developing nervous system in various vertebrate species ([WMS] and [Y]). In the developing retina, spontaneous neuronal activity can be monitored in the ganglion cell layer and it exhibits complicated spatiotemporal patterns called retinal waves ([MWBS] and [C]). It is known that a synaptically connected network of amacrine cells and ganglion cells in retina produces these waves ([WCSS] and [FWSWS]).

Feller et al ([FBARS]) have created a computational two layer model of the developing retina which reproduces the spatiotemporal properties (retinal waves) and suggests a mechanism by which the retinal circuitry can generate these patterns.

The model in [BFSR] and [FBARS] uses instructions much like those used in cellular automata instead of using the more common integrate-and-fire, Hodgkin-Huxley or firing rate techniques to produce the main mechanisms. In this dissertation, we have developed a firing rate model that simulates the results in [BFSR] and [FBARS]. The model is simplified to be only one-dimensional.

An outline of this dissertation is as follows. In Chapter 2, we briefly introduce concepts on mathematical neuroscience as well as some of important mathematical models. We include Hodgkin-Huxley, FitzHugh Nagumo, and Morris-Lecar models as well as an integro-differential equation model for networks. In Chapter 3, we introduce the exponential Euler scheme and provide a rigorous error analysis of the scheme as well as a second-order accurate extension of it in the case of ODE system neuron models. A brief qualitative and stability analysis of this scheme is furnished. Next, we analyze the exponential Euler scheme when it is applied to integro-differential models and show that the scheme is first-order accurate. At the end of this chapter we suggest a fully discrete approximation method for time-dependent partial differential equations which uses the exponential Euler scheme for the time discretization. We also provide rather extensive computational results for

the scheme in this chapter. In Chapter 4, we introduce a firing rate mathematical model that reproduces the spatiotemporal properties of retinal waves as well as a derivation of the model and some computational results.

## Chapter 2

# Mathematical Neuroscience

In this chapter, we briefly discuss some basic concepts in neuroscience. This will help to understand the mathematical models in Chapters 3 and 4. More information and details can be found in [Z], [KS], [F], and [T].

### 2.1 Neuron and Action Potential

The basic unit of the nervous system is the neuron. Most neurons consist of three parts: the cell body (or soma), the dendrites, and the axon. Figure 2.1 shows the structures of a typical neuron. The dendrites receive incoming signals from other neurons. These signals are transmitted along the axon to other neurons. At the

end of an axon, there are cellular junctions, called synapses, where the cells can communicate with each other.

Each neuron is surrounded by a cell membrane that separates the cell from the external environment. Many ions such as  $Na^+$ ,  $K^+$ ,  $Ca^{2+}$ , and  $Cl^-$  are dissolved in the intracellular and extracellular environments. Usually the ionic concentrations in and out of the cells are different. For example, the intracellular concentration of the potassium ions is higher than that outside of the cell, while the intracellular concentrations of sodium and calcium ions are lower than their extracellular concentrations. There are many ion channels and pumps in the cell membrane that maintain these concentration differences of the ions between the inside and outside of the cells. Since the ion concentrations on the inside and the outside of the cells are different, there is a potential difference across the membrane.

When the cell is stimulated (if enough applied current occurs so that the membrane potential reaches a threshold level), the membrane potential goes through a dramatic change, which is called an action potential. Neurons communicate with each other by generating and transmitting these action potentials. During the action potential, the permeability of the cell membrane to the ions is changed. For instance, during the action potential, the sodium channels are open allowing the sodium ions outside of the cell to flow into the cytoplasm. This results in a rapid rise in the membrane potential. After that, the sodium channels are closed and

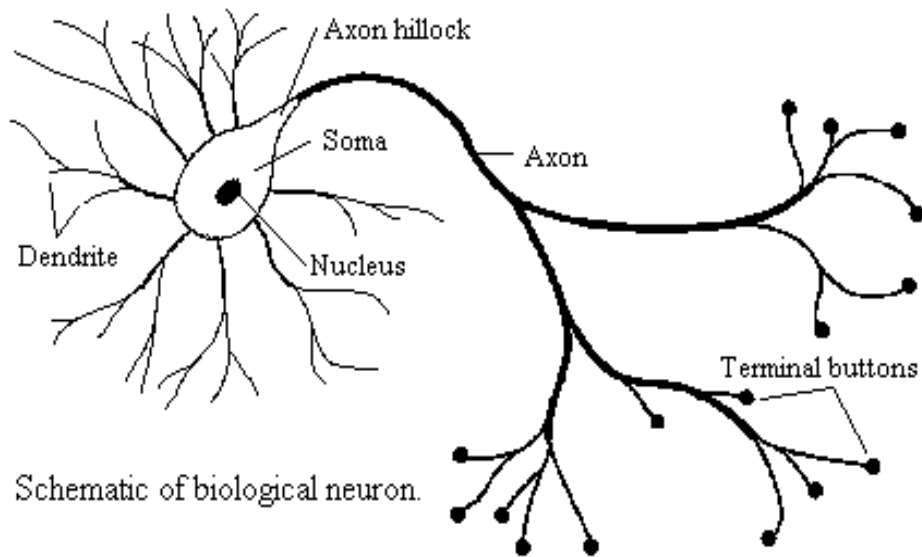


Figure 2.1: Schematic diagram of biological neuron

the potassium channels are open so that the potassium ions flow out of the cell. This brings the membrane potential back to the resting potential (Figure 2.2). It is important to understand that the sodium channels act very quickly while the potassium channels act slowly.

After firing an action potential, a nerve cell is incapable, for a certain amount of time called a refractory period, of firing another action potential and the sodium and potassium pumps move sodium and potassium ions in and out of the cell until the membrane potential reaches the resting membrane potential.

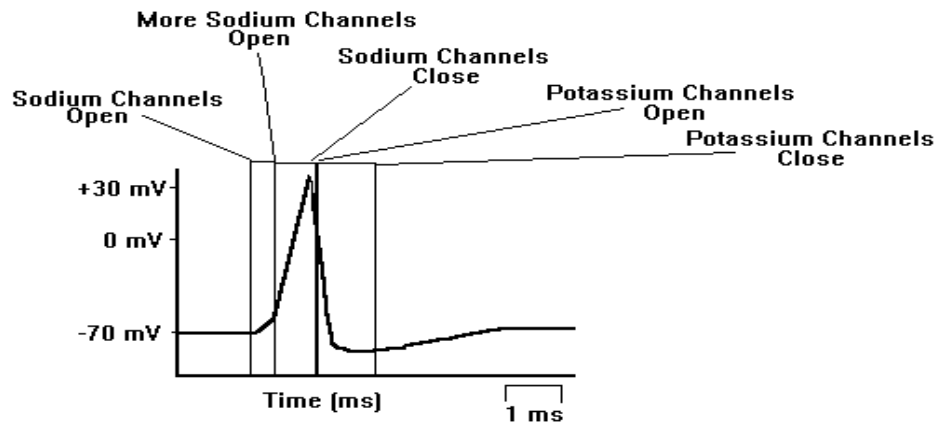


Figure 2.2: Action Potential

## 2.2 Morris-Lecar Model

Mathematical modeling took a major step forward in 1952; Alan L. Hodgkin and Andrew F. Huxley developed the first quantitative model of electrical activity of a squid giant axon in a series of five articles ([HHa], [HHb], [HHc], [HHd], and [HH]). They were awarded the 1963 Nobel Prize in physiology and medicine. Although their model was originally developed to describe the action potential in the giant axon of a squid, it became the basic equation for modeling of electrical activity of cells and the study of excitability.

The Morris-Lecar model is a Hodgkin-Huxley type model that contains a system

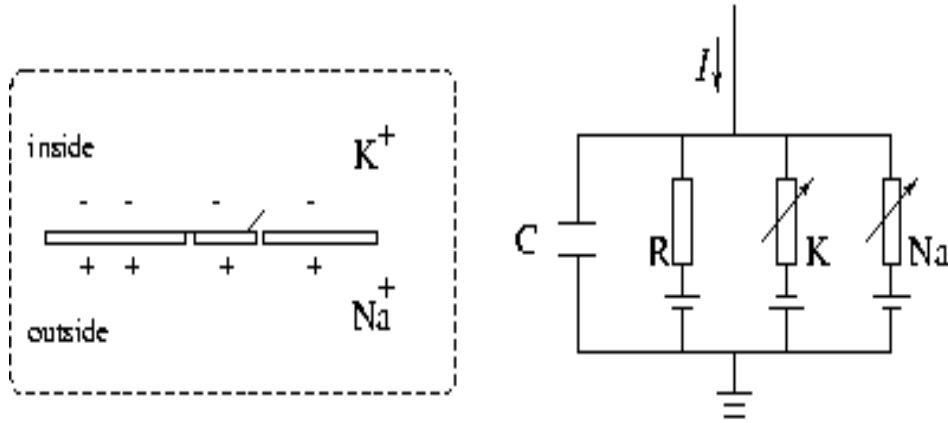


Figure 2.3: Schematic diagram for the Hodgkin-Huxley model.

of two differential equations. This model is originally formulated to describe electrical activity for a barnacle muscle fiber. The Morris-Lecar model is defined by the following system of differential equations:

$$\begin{aligned}
 C \frac{dV}{dt} &= -g_{Ca} m_{\infty} (V - V_{Ca}) - g_K w (V - V_K) - g_L (V - V_L) + I \\
 \frac{dw}{dt} &= \frac{(w_{\infty} - w)}{\tau}.
 \end{aligned}
 \tag{2.1}$$

The basic idea of this equation is obtained from Ohm's law,

$$V = IR$$

where  $V$  is the potential difference (voltage) between two points which includes a

resistance  $R$ . For biological work, it is often written as

$$I = gV$$

where the conductance  $g = \frac{1}{R}$ . In neuroscience,  $V$  represents the potential difference between the membrane potential and the resting potential, and  $I$  is the current flowing across the membrane. We consider the cell membrane as a capacitor in parallel with ionic currents. In this model, there are a delayed rectifier potassium current, a fast activating calcium current and a leak current. The Ohm's law gives the potassium current as  $I_K = g_K w(V - V_K)$  where the potassium conductance is  $g_K w$  and  $(V - V_K)$  is a driving potential.  $g_K$  is the maximum potassium conductance and  $w$ , known as a recovery variable, represents the fraction of open potassium channels. Similarly, the calcium current is represented as  $I_{Ca} = g_{Ca} m_\infty (V - V_{Ca})$ . Here  $m_\infty$  is the percentage of open calcium channels and  $g_{Ca}$  is the maximum calcium conductance.

The functions

$$\begin{aligned} m_\infty(V) &= 0.5 \cdot [1 + \tanh(\frac{V - \nu_1}{\nu_2})], \\ w_\infty(V) &= 0.5 \cdot [1 + \tanh(\frac{V - \nu_3}{\nu_4})], \\ \tau(V) &= (\cosh(\frac{V - \nu_3}{2 \cdot \nu_4}))^{-1}, \end{aligned}$$

are the equilibrium open fractions for the calcium current, the potassium current, and the activation time constant for a delayed rectifier, respectively. Here,

$C = 20\mu mF/cm^2$ ,  $g_{Ca} = 4.4mS/cm^2$ ,  $g_K = 8mS/cm^2$ ,  $g_L = 2mS/cm^2$ ,  $\nu_1 = -1.2mV$ ,  $\nu_2 = 18mV$ ,  $\nu_3 = 2mV$ ,  $\nu_4 = 30mV$ ,  $V_K = -84mV$ ,  $V_{Ca} = 120mV$ , and  $V_L = -80mV$ .

### 2.3 FitzHugh-Nagumo Equation

The FitzHugh Nagumo equation is a simplification of the Hodgkin-Huxley model that consists of two variables, one fast and one slow. The fast variable is the excitable variable while the slow variable is called the recovery variable. The parameter  $\epsilon$  is introduced in order to control the speed of one variable relative to the other variable. Phase plane techniques can be used to analyze this model (see [KS]).

The FitzHugh Nagumo model is defined by the following system of differential equations with the dimensionless variables:

$$\begin{aligned}
 \epsilon \frac{dv}{dt} &= f(v) - w - w_0 \\
 \frac{dw}{dt} &= v - \gamma w - v_0
 \end{aligned}$$

where  $f(v) = Av(v - \alpha)(1 - v)$  with  $0 < \alpha < 1$ .

The generalized FitzHugh Nagumo model is defined by the following system of

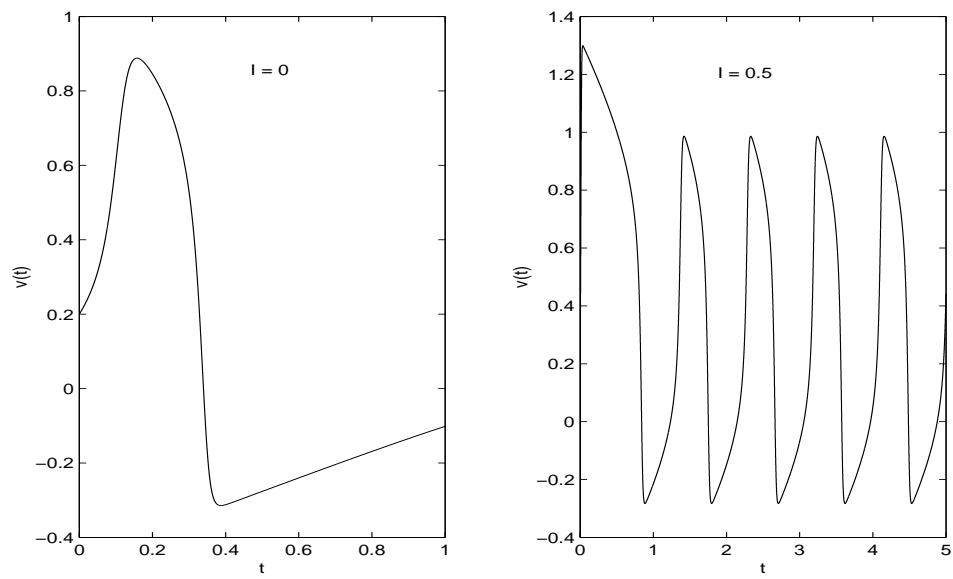


Figure 2.4: Solutions of FitzHugh Nagumo system (2.2 and 3.27) with  $\epsilon=0.014$  where  $I=0$  (left) and  $I=0.5$  (right)

differential equations:

$$\begin{aligned}\epsilon \frac{dv}{dt} &= f(v, w) + I \\ \frac{dw}{dt} &= g(v, w)\end{aligned}\tag{2.2}$$

where the nullcline  $f(v, w) = 0$  resembles the cubic shape and the nullcline  $g(v, w) = 0$  has precisely one intersection with  $f(v, w) = 0$ . See Figure 2.4 for pictures of the solution  $v$ .

## 2.4 Hodgkin-Huxley Model

The Hodgkin-Huxley model consists of four differential equations. One of the equations of the model describes the evolution of the membrane potential, and the rest of the equations represents the properties of the ionic channels. The Hodgkin-Huxley model can be written as follows:

$$\begin{aligned}C \frac{dv}{dt} &= -g_K n^4 (v - v_K) - g_{Na} m^3 h (v - v_{Na}) - g_L (v - v_L) + I_{app}, \\ \frac{dm}{dt} &= -\frac{(m - m_\infty)}{\tau_m}, \\ \frac{dn}{dt} &= -\frac{(n - n_\infty)}{\tau_n}, \\ \frac{dh}{dt} &= -\frac{(h - h_\infty)}{\tau_h}.\end{aligned}$$

Here,  $v$  represents the membrane potential and each term in the first equation represents the ionic currents.  $v_K$ ,  $v_{Na}$ , and  $v_L$  represent the resting potentials of the ions and  $g_K n^4$ ,  $g_{Na} m^3 h$ , and  $g_L$  are the conductances of the ions. Also,  $m$  and  $n$  are the activation gating variables, and  $h$  represents the inactivation. All are functions of  $v$ . These gate variables obey the equations of two-state channel models and vary between zero and one with voltage dependent functions,  $\tau_m$ ,  $\tau_n$ , and  $\tau_h$  (See [KS]).

## 2.5 Integro-Differential Equations

Synaptically coupled neuronal activity models are often described by integro-differential equations (see [TEY], for instance). Consider the following integro-differential equation which, loosely, models a one dimensional network of neurons connected by synapses in nondimensionalized form ( see page 213 in [PE], for instance),

$$u_t = -u - w * g(u)(u - u_R) + f \quad \text{and} \quad u(\cdot, 0) = u_0 \quad (2.3)$$

where  $u = u(x, t)$  usually represents an averaged membrane potential at point  $x$  (spatial location) and time  $t$ . Here,  $u_R$  is a nondimensionalized reversal potential, the second term,  $w * g(u)(u - u_R)$  represents the synaptic currents. The symbol  $*$

is for convolution over the spatial domain and is defined by

$$w * g(u) = \int_{-\infty}^{\infty} w(x-y)g(u(y,t)) dy$$

where  $w$  is the distance dependent strength (or weight) of synaptic interaction. The function  $w$  is often defined on  $(-\infty, \infty)$ , bounded, even and normalized such that

$$\int_{\mathbb{R}} w dx = 1.$$

For example,  $w$  might be defined to be a Gaussian ([PE]) or a Mexican hat ([LTGE]).

The firing rate function  $g(u)$  is nonnegative, monotone increasing and  $f = f(x, t)$  includes equations for ionic channels and gates as well as the applied current. Interest in these models focuses on traveling wave solutions and stationary bump solutions ([PE], [TEY] and [LTGE]).

## Chapter 3

# Error Analysis of Exponential Euler Method

In this section, we introduce the Exponential Euler method, and present the error analysis of the scheme and a second order modification. Also, we provide an error estimate of the method applied to the basic integro-differential equation model that often describes synaptically coupled neuronal networks.

### 3.1 Derivation and Motivation

Consider the initial value problem:

$$y' = A(y) - B(y)y, \quad y(0) = y_0 \tag{3.1}$$

where, in general,  $A(y)$  and  $y$  will be vectors and  $B(y)$  will be a diagonal matrix. In neuroscience, one of the components of  $y$  is the voltage (membrane potential) of a cell and is dependent on time (and often spatial location too). The other components will represent the states of the various ion channels. Most of the initial value problems that arise in neuroscience take the form of equation (3.1). For example, consider the Morris-Lecar equations introduced in previous chapter (see [ML] or [T]). To place the Morris-Lecar equations in the form (3.1), we set

$$y = \begin{pmatrix} v \\ w \end{pmatrix}, \quad A(y) = \begin{pmatrix} \frac{1}{C}(g_L v_L + g_K w v_K + g_{Ca} m_\infty(v) v_{Ca} + I) \\ w_\infty(v)/\tau(v) \end{pmatrix},$$

and

$$B(y) = \begin{bmatrix} \frac{1}{C}(g_L + g_k w + g_{Ca} m_\infty(v)) & 0 \\ 0 & \tau(v)^{-1} \end{bmatrix}.$$

The exponential Euler method could also be applied to the ionic current equations

that arise in cardiology (see [KS] or [SLT]).

The derivation of the exponential Euler scheme follows from the fact that there would be an exact solution for the differential equation if the functions  $A$  and  $B$  were constant. Partition the interval  $[0, T]$  uniformly and let  $t_n = nh$  and  $h = T/N$ . Also let  $I_{n+1} = [t_n, t_{n+1}]$ . The exponential Euler scheme is

$$y_{n+1} = e^{-B(\tilde{y}_n)h} y_n + B(\tilde{y}_n)^{-1} (I - e^{-B(\tilde{y}_n)h}) A(\tilde{y}_n). \quad (3.2)$$

where in the standard scheme, the extrapolation is  $\tilde{y}_n = y_n$ . Since  $B$  is a diagonal matrix,  $B^{-1}(\tilde{y}_n)$  and  $e^{-B(\tilde{y}_n)h}$  are straightforward to compute. By setting the extrapolation

$$\tilde{y}_n = y_n + \frac{h}{2} (A(y_n) - B(y_n)y_n), \quad (3.3)$$

we will show that a second order accurate scheme results.

## 3.2 Error Estimation for the Basic Exponential Euler Scheme:

In this section we focus on the error analysis for the exponential Euler method. As we mentioned earlier and noted in [BB] this has not been done before. The basic

exponential Euler scheme is first order accurate and our error estimation allows us to create second order extensions which we present in Theorem 3.3.2.

In order to analyze the error of the scheme, we need the following hypotheses. We assume that the solution of the IVP (3.1) has two continuous derivatives; thus there exists a positive constant  $M$  so that

$$\| D^j y \|_{L^\infty(0,T)} \leq M \quad \text{for } j = 0, 1, \text{ and } 2. \quad (3.4)$$

This is reasonable for models from neuroscience since in most cases,  $y$  represents a bounded quantity such as the membrane potential of a cell (Action potentials, though representing sharp changes in behavior, are generally smooth in Hodgkin-Huxley models.). We also assume  $A$  and  $B$  are continuously differentiable.

**Lemma 3.2.1** *Let  $w$  be a continuously differentiable function on  $I_{n+1}$  which is bounded with a bounded first derivative. Then*

$$|A(w(t_n)) - \frac{1}{h} \int_{I_{n+1}} A(w(s)) ds| \leq Ch \quad (3.5)$$

$$|B(w(t_n)) - \frac{1}{h} \int_{I_{n+1}} B(w(s)) ds| \leq Ch \quad (3.6)$$

where  $C$  is positive constant that is independent of  $h$ .

**Proof:** Both estimates follow by rewriting the first term as an integral (e.g.

$A(w(t_n)) = \frac{1}{h} \int_{I_{n+1}} A(w(t_n)) ds$  and then using the Taylor expansion

$$A(w(s)) - A(w(t_n)) = A'(y(\xi))y'(\xi)(s - t_n). \blacksquare$$

We are now in a position to state and prove our main theorem,

**Theorem 3.2.2** *Let  $y$  be the solution of (3.1) and  $y_n$  be the values obtained from the method (3.2) for  $n = 1, 2, \dots, N$  with  $\tilde{y}_n = y_n$  on  $I_{n+1}$ . Then,*

$$\|y(t_n) - y_n\|_\infty \leq Ch \quad \text{for } n = 1, 2, \dots, N.$$

**Proof:** We redefine  $A$  and  $B$  to create a numerical approximation, the  $z_n$ , which is guaranteed to be bounded; we eventually show that  $z_n = y_n$  for all  $n$ . Let  $\tilde{A}(z) = A(z)$  for  $\|z\|_{L^\infty(0,T)} \leq M + 1$  and extend  $\tilde{A}(z)$  outside of  $[-(M + 1), M + 1]$  so that

$$\|\tilde{A}^{(j)}\|_{L^\infty(\mathbb{R})} \leq K \quad \text{for } j = 0 \text{ and } 1. \quad (3.7)$$

Similarly define  $\tilde{B}(z)$  so that for  $j = 0$  and  $1$ ,

$$\tilde{B}(z) = B(z) \quad \text{for } \|z\|_{L^\infty(0,T)} \leq M + 1 \quad \text{and} \quad \|\tilde{B}^{(j)}\|_{L^\infty(\mathbb{R})} \leq K. \quad (3.8)$$

Since  $y$  is bounded by  $M$ , it is also the solution of the differential equation with  $A$  and  $B$  replaced by  $\tilde{A}$  and  $\tilde{B}$ . Let  $z_{n+1}$  be defined by

$$z_{n+1} = e^{-\tilde{B}(z_n)h} z_n + \tilde{B}(z_n)^{-1} (I - e^{-\tilde{B}(z_n)h}) \tilde{A}(z_n).$$

for  $n = 1, 2, \dots, N$  and  $z_0 = y_0$ . We will now show that

$$\| y(t_n) - z_n \|_\infty \leq Ch. \quad (3.9)$$

This will complete the proof since

$$\| z_n \|_\infty = \| y(t_n) + z_n - y(t_n) \|_\infty \leq \| y(t_n) \|_\infty + \| z_n - y(t_n) \|_\infty \leq M + Ch$$

and so for  $h \leq \frac{1}{C}$ , we have  $\| z_n \|_\infty \leq M + 1$ . Then we have  $y_n = z_n$  since  $\tilde{A}(z_n) = A(z_n)$  and  $\tilde{B}(z_n) = B(z_n)$  for all  $n$ . Therefore,  $\| y(t_n) - y_n \|_\infty \leq Ch$ .

We now prove (3.9). Let  $\tau_{n+1}$  be the local truncation error on  $I_{n+1}$  defined, as is customary, by inserting the true solution  $y$  into the numerical scheme (3.2) (with  $y(t_n)$  as the extrapolation substituted in the  $A$  and  $B$  functionals),

$$y(t_{n+1}) = e^{-B(y(t_n))h} y(t_n) + B(y(t_n))^{-1} \left( I - e^{-B(y(t_n))h} \right) A(y(t_n)) + \tau_{n+1}.$$

or

$$y(t_{n+1}) = e^{-B(y(t_n))h} y(t_n) + \int_{I_{n+1}} e^{-\int_t^{t_{n+1}} B(y(t_n)) ds} A(y(t_n)) dt + \tau_{n+1}.$$

Then

$$\tau_{n+1} = y(t_{n+1}) - e^{-B(y(t_n))h} y(t_n) - \int_{I_{n+1}} e^{-\int_t^{t_{n+1}} B(y(t_n)) ds} A(y(t_n)) dt$$

$$\begin{aligned}
&= e^{-\int_{I_{n+1}} B(y(s)) ds} y(t_n) + \int_{I_{n+1}} e^{-\int_t^{t_{n+1}} B(y(s)) ds} A(y(t)) dt \\
&\quad - e^{-B(y(t_n))h} y(t_n) - \int_{I_{n+1}} e^{-\int_t^{t_{n+1}} B(y(t_n)) ds} A(y(t_n)) dt \\
&= \left[ e^{-\int_{I_{n+1}} B(y(s)) ds} - e^{-B(y(t_n))h} \right] y(t_n) \\
&\quad + \int_{I_{n+1}} \left[ e^{-\int_t^{t_{n+1}} B(y(s)) ds} A(y(t)) - e^{-\int_t^{t_{n+1}} B(y(t_n)) ds} A(y(t_n)) \right] dt \\
&= U + V.
\end{aligned}$$

Now, using (3.6) of the lemma 3.1,

$$\begin{aligned}
\| U \|_\infty &= \left\| \left( e^{-\int_{I_{n+1}} B(y(s)) ds} - e^{-B(y(t_n))h} \right) y(t_n) \right\|_\infty \\
&= \left\| e^{-\xi} \left( B(y(t_n))h - \int_{I_{n+1}} B(y(s)) ds \right) y(t_n) \right\|_\infty \\
&\leq Ch^2.
\end{aligned}$$

We used the meanvalue theorem on the second step with  $\xi$  a diagonal matrix and  $\xi_{ii}$  in between  $(B(y(t_n))h)_{ii}$  and  $\left( \int_{I_{n+1}} B(y(s)) ds \right)_{ii}$  for  $i = 1, 2, \dots, d$ . For the second term  $V$ , we have

$$\begin{aligned}
\| V \|_\infty &= \left\| \int_{I_{n+1}} \left[ e^{-\int_t^{t_{n+1}} B(y(s)) ds} A(y(t)) - e^{-\int_t^{t_{n+1}} B(y(t_n)) ds} A(y(t)) \right. \right. \\
&\quad \left. \left. + e^{-\int_t^{t_{n+1}} B(y(t_n)) ds} (A(y(t)) - A(y(t_n))) \right] dt \right\|_\infty \\
&\leq \left\| \int_{I_{n+1}} e^{-\xi} \left( B(y(t_n))h - \int_t^{t_{n+1}} B(y(s)) ds \right) A(y(t)) dt \right\|_\infty \\
&\quad + \left\| \int_{I_{n+1}} e^{-\int_t^{t_{n+1}} B(y(t_n)) ds} (A(y(t)) - A(y(t_n))) dt \right\|_\infty. \quad (3.10)
\end{aligned}$$

Here, we also used the Mean Value Theorem on the second step with  $\xi_{ii}$  in between  $\left( \int_t^{t_{n+1}} B(\tilde{y}_n)h ds \right)_{ii}$  and  $\left( \int_t^{t_{n+1}} B(y(s)) ds \right)_{ii}$  for  $i = 1, 2, \dots, d$ . For the first term

on the right of the expression above, we have

$$\begin{aligned}
& \left\| \int_{I_{n+1}} e^{-\xi} \left( B(y(t_n))h - \int_t^{t_{n+1}} B(y(s)) ds \right) A(y(t)) dt \right\|_\infty \\
&= \left\| \int_{I_{n+1}} e^{-\xi} \left( \int_t^{t_{n+1}} (B(y(t_n)) - B(y(s))) ds \right) A(y(t)) dt \right\|_\infty \\
&\leq O(h^3)
\end{aligned}$$

since for  $t \leq s \leq t_{n+1}$ ,

$$|B(y(t_n)) - B(y(s))| = |B'(\eta)(y(s) - y(t_n))| \leq Ch.$$

And using (3.5) of the lemma 3.1, the second term on the right of (3.10) is  $O(h^2)$ .

Thus, we can conclude

$$\|V\|_\infty \leq Ch^2$$

and therefore, we have

$$\|\tau_{n+1}\|_\infty \leq Ch^2.$$

So, letting  $E_{n+1} = y(t_{n+1}) - z_{n+1}$ , we have

$$\begin{aligned}
E_{n+1} &= e^{-B(y(t_n))h} y(t_n) + \int_{I_{n+1}} e^{-\int_t^{t_{n+1}} B(y(t_n)) ds} A(y(t_n)) dt \\
&\quad - e^{-\tilde{B}(z_n)h} z_n - \int_{I_{n+1}} e^{-\int_t^{t_{n+1}} \tilde{B}(z_n) ds} \tilde{A}(z_n) dt + \tau_{n+1}. \quad (3.11)
\end{aligned}$$

We now estimate the difference of the first and the third terms;

$$\begin{aligned}
& \left\| e^{-B(y(t_n))h} y(t_n) - e^{-\tilde{B}(z_n)h} z_n \right\|_\infty \\
&\leq \left\| (e^{-B(y(t_n))h} - e^{-\tilde{B}(z_n)h}) y(t_n) + e^{-\tilde{B}(z_n)h} (y(t_n) - z_n) \right\|_\infty
\end{aligned}$$

$$\begin{aligned}
&\leq h \| e^\eta (\tilde{B}(z_n) - B(y(t_n))) y(t_n) \|_\infty + \| (I - h e^\xi \tilde{B}(z_n)) E_n \|_\infty \\
&\leq (1 + Ch) \| E_n \|_\infty
\end{aligned}$$

using  $B(y(t_n)) = \tilde{B}(y(t_n))$ . Here,  $\eta_{ii}$  is between  $(\tilde{B}(z_n))_{ii}$  and  $(B(y_n))_{ii}$  and  $\xi_{ii}$  is between 1 and  $(\tilde{B}(z_n))_{ii}$  for  $i = 1, 2, \dots, d$ . Similarly, estimating the difference of the second and the fourth terms in (3.11) by adding and subtracting  $e^{-\int_t^{t_{n+1}} \tilde{B}(z_n) ds} A(y(t_n)) ds$ , we obtain

$$\begin{aligned}
&\| \int_{I_{n+1}} e^{-\int_t^{t_{n+1}} B(y(t_n)) ds} A(y(t_n)) dt - \int_{I_{n+1}} e^{-\int_t^{t_{n+1}} \tilde{B}(z_n) ds} \tilde{A}(\tilde{z}_n) dt \|_\infty \\
&\leq (1 + Ch) \| E_n \|_\infty
\end{aligned}$$

using the fact that  $\tilde{B}(y(t_n)) = B(y(t_n))$  and  $\tilde{A}(y(t_n)) = A(y(t_n))$ . So, we have from (3.11) and our estimates

$$\| E_{n+1} \|_\infty \leq (1 + Ch) \| E_n \|_\infty + \| \tau_{n+1} \|_\infty .$$

We now apply the above inequality for  $n, n-1, \dots, 1$ . Since  $\| \tau_{n+1} \|_\infty = O(h^2)$ , we have

$$\| E_n \|_\infty \leq (1 + Ch)^n \| E_0 \|_\infty + O(h) \leq C \| E_0 \| + O(h). \blacksquare$$

That completes our proof. Hence, the basic exponential Euler method is first order accurate.

### 3.3 Error Estimate for the Modified Exponential Euler Scheme

In this section, we introduce a modified exponential Euler scheme which is the second order accurate. Here, we used the basic midpoint method to define the  $\tilde{y}_n$  in equation (3.3). To prove the second order accuracy of the modified scheme, we need the following lemma.

**Lemma 3.3.1** *Let  $y$  be the solution of (3.1). Suppose (3.4) holds and  $A$ ,  $B$  and their first and second order derivatives are bounded. Then,*

$$\| A(y(t_n) + \frac{h}{2}f(y(t_n))) - \frac{1}{h} \int_{I_{n+1}} A(y(s)) ds \|_{\infty} \leq Ch^2 \quad (3.12)$$

$$\| B(y(t_n) + \frac{h}{2}f(y(t_n))) - \frac{1}{h} \int_{I_{n+1}} B(y(s)) ds \|_{\infty} \leq Ch^2 \quad (3.13)$$

where  $C$  is positive constant that is independent of  $h$  but may depend on the bounded quantities (e.g.  $A$ ,  $A'$ ,  $B$ , ...). Here  $f(y) = A(y) - B(y)y$ .

**Proof:** We can easily show (3.12), using Taylor expansion with the assumption (3.4) and the boundedness of the derivatives of the function  $A$ ;

$$\begin{aligned} & A(y(t_n) + \frac{h}{2}f(y(t_n))) - \frac{1}{h} \int_{I_{n+1}} A(y(s)) ds \\ = & A(y(t_n)) + \frac{h}{2}f(y(t_n))A'(y(t_n)) \end{aligned}$$

$$\begin{aligned}
& -\frac{1}{h} \int_{I_{n+1}} [A(y(t_n)) + A'(y(t_n))y'(t_n)(s - t_n)] ds + O(h^2) \\
& = O(h^2).
\end{aligned}$$

The last step follows since  $\int_{I_{n+1}} (s - t_n) ds = \frac{h^2}{2}$ ,  $\frac{1}{h} \int_{I_{n+1}} ds = 1$  and  $y'(t_n) = f(y(t_n))$ .

Similarly, we can prove (3.13). ■

The following theorem shows that the modified exponential Euler method using the basic midpoint scheme is second order accurate.

**Theorem 3.3.2** *Let  $y$  be the solution of (3.1) and  $y_n$  be the values obtained from the method (3.2) with  $\tilde{y}_n$  defined as in (3.3) for  $n = 1, 2, \dots, N$ . Suppose (3.4), (3.12) and (3.13) hold and second order derivatives of the functions  $A$  and  $B$  are bounded. Then*

$$\|y(t_n) - y_n\|_\infty \leq Ch^2 \quad \text{for } n = 1, 2, \dots, N.$$

**Proof:** The proof of this theorem is very similar to that of Theorem 3.2.2. We only need to show that the truncation error of the modified exponential Euler scheme is  $O(h^3)$ . Let  $\tau_{n+1}$  be the local truncation error on  $I_{n+1}$ , then we have

$$\begin{aligned}
\tau_{n+1} &= e^{-\int_{I_{n+1}} B(y(s)) ds} y(t_n) + \int_{I_{n+1}} e^{-\int_t^{t_{n+1}} B(y(s)) ds} A(y(t)) dt \\
&\quad - e^{-B(\tilde{y}_n)h} y(t_n) - \int_{I_{n+1}} e^{-\int_t^{t_{n+1}} B(\tilde{y}_n) ds} A(\tilde{y}_n) dt \\
&= \left[ e^{-\int_{I_{n+1}} B(y(s)) ds} - e^{-B(\tilde{y}_n)h} \right] y(t_n)
\end{aligned}$$

$$\begin{aligned}
& + \int_{I_{n+1}} \left[ e^{-\int_t^{t_{n+1}} B(y(s)) ds} A(y(t)) - e^{-\int_t^{t_{n+1}} B(\tilde{y}_n) ds} A(\tilde{y}_n) \right] dt \\
& = U_2 + V_2.
\end{aligned}$$

Now, using (3.13) of the lemma 3.3.1 and the Mean Value Theorem,

$$\| U_2 \|_\infty \leq Ch^3$$

. For the second term  $V_2$ , we have

$$\begin{aligned}
\| V_2 \|_\infty & \leq \left\| \int_{I_{n+1}} e^{-\xi} \left( B(\tilde{y}_n)h - \int_t^{t_{n+1}} B(y(s)) ds \right) A(y(t)) dt \right\|_\infty \\
& \quad + \left\| \int_{I_{n+1}} e^{-\int_t^{t_{n+1}} B(\tilde{y}_n) ds} (A(y(t)) - A(\tilde{y}_n)) dt \right\|_\infty. \quad (3.14)
\end{aligned}$$

We also used the mean value theorem. For the first term on the right of the expression above, we have

$$\begin{aligned}
& \left\| \int_{I_{n+1}} e^{-\xi} \left( B(\tilde{y}_n)h - \int_t^{t_{n+1}} B(y(s)) ds \right) A(y(t)) dt \right\|_\infty \\
& = \left\| \int_{I_{n+1}} e^{-\xi} \left( \int_t^{t_{n+1}} (B(\tilde{y}_n) - B(y(s))) ds \right) A(y(t)) dt \right\|_\infty \\
& \leq O(h^3)
\end{aligned}$$

since for  $t \leq s \leq t_{n+1}$ ,

$$\begin{aligned}
\| B(\tilde{y}_n) - B(y(s)) \|_\infty & = \| B'(\eta)[y(s) - y(t_n) - \frac{h}{2}(A(y(t_n)) - B(y(t_n))y(t_n))] \|_\infty \\
& \leq Ch.
\end{aligned}$$

And using (3.12) of the lemma 3.3.1, the second term on the right of (3.14) is  $O(h^3)$ .

Therefore, we can conclude

$$\| V_2 \|_\infty \leq Ch^3.$$

Hence, we have

$$\| \tau_{n+1} \|_{\infty} \leq Ch^3.$$

That completes our proof. ■

Numerical results will be presented in the Section 3.7 that will provide an explicit example of this.

### 3.4 Qualitative Analysis of the Scheme

In this chapter, we examine the dynamics and stability of the exponential Euler scheme. In general, to test the stability of a method, the scalar test equation,

$$y' = \lambda y, \quad \text{with } y(0) = 1 \quad \text{where } \operatorname{Re}(\lambda) \leq 0$$

is used. However, the exponential Euler method solves the above test equation exactly making it already quite stable relative to the usual criterion. To explore the schemes stability properties a little further, inspired by the work in [I], we used the logistic equation,

$$y' = \beta y(1 - y), \quad \text{with } y(0) = y_0 \quad \text{where } \beta > 0 \quad \text{and real.} \quad (3.15)$$

as a test equation.

First, we quickly summarize some basic ideas used in a qualitative analysis of an ODE. For

$$y' = f(y) \quad \text{with} \quad y(0) = y_0. \quad (3.16)$$

We define that  $\hat{y}$  is a *fixed point* of (3.16) if  $f(\hat{y}) = 0$ . To examine the stability of the differential equation (3.16) at the fixed points, it is customary to set  $\epsilon(t) = y(t) - \hat{y}$  and then

$$\epsilon'(t) = f(y) - f(\hat{y}) \doteq f'(\hat{y})\epsilon(t).$$

And we have a following definition for the stability of the fixed point of (3.16); we say the fixed point of (3.16) is *stable* if  $f'(\hat{y}) < 0$ .

**Example 3.4.1** (Logistic Equation)

In the case of the logistic equation (3.15), the fixed points are 0 and 1 and, since

$$f'(\hat{y}) = \beta(1 - 2\hat{y}).$$

the fixed point  $\hat{y} = 1$  is stable. It turns out that  $\lim_{t \rightarrow \infty} y(t) = 1$  if  $y_0 > 0$ .

To study the stability of numerical methods near fixed points, we examine the map

$$y_{n+1} = \Phi(y_n).$$

We also define  $\tilde{Y}$  as a fixed point (rest point) of the numerical method if  $\tilde{Y} = \Phi(\tilde{Y})$ , and we say that the numerical method is *stable* in the neighborhood of the fixed point  $\tilde{Y}$  if  $|\Phi_y(\tilde{Y})| < 1$ .

**Example 3.4.2** (Forward Euler Scheme)

The forward Euler method is the conventional explicit method;

$$y_{n+1} = y_n + hf(y_n). \quad (3.17)$$

If we let  $\Phi(y) = y + hf(y)$ , then (3.17) can be written as  $y_{n+1} = \Phi(y_n)$ . To find the fixed point of the forward Euler method, we let  $\tilde{Y} = \Phi(\tilde{Y}) = \tilde{Y} + hf(\tilde{Y})$ . Then,  $f(\tilde{Y}) = 0$ . On the other hand, the fixed points  $\hat{y}$  of the differential equation (3.16) satisfy  $f(\hat{y}) = 0$ . Therefore, the forward Euler scheme has the same fixed points as the differential equation. For instance, the fixed points of the forward Euler method are 0 and 1 in the case of logistic equation (3.15).

To analyze the stability of the method applied to (3.15), we find that  $\Phi'(\hat{Y}) = 1 + h\beta(1 - 2\hat{Y})$ . Therefore, for the method to be stable at  $\hat{Y} = 1$  we must have  $h < 2/\beta$  (restriction on the step size  $h$ .) ■

We carry out similar calculations for the exponential Euler scheme; here

$$\Phi(y_n) = y_n e^{-B(y_n)h} + \frac{A(y_n)}{B(y_n)}(1 - e^{-B(y_n)h}).$$

Solving  $\Phi(\hat{Y}) = \hat{Y}$  for  $\hat{Y}$ , we have  $\hat{Y} = 1$  or  $\hat{Y} = 0$ . So, the exponential Euler scheme also has the same fixed points as those of the logistic equation.

To examine the stability of the exponential Euler scheme applied to the logistic equation near  $\hat{Y} = 1$ , we find

$$\Phi'(\hat{Y}) = e^{-\beta\hat{Y}h}(1 - \beta\hat{Y}h + \beta h).$$

Since  $\Phi'(1) = e^{-\beta h}$  and  $\beta > 0$  we have  $\Phi_y(1) \leq 1$  for all positive number  $h$ . This allows us to conclude there are no restrictions on the step size  $h$ . In Figure 3.1, we display the results of several computations with  $\beta = 0.5$  and  $h = 5$ . These plots confirm that the forward Euler method is unstable while the exponential Euler scheme is not.

**Remark:** We have also applied this analysis to the second order exponential Euler introduced in Section 2.2. In that case, the method has three fixed point,  $\hat{Y} = 0, 1$ , and  $1 + 2/(h\beta)$ . However, studying  $\Phi_y$  as above we found that the method is unstable at the extraneous fixed point,  $1 + 2/(h\beta)$ . Thus, in computations, the numerical solution will still tend to 1.

### 3.5 Application to an Integro-Differential Equation

In this section, we apply the exponential Euler scheme to the following integro-differential equation that was introduced in Chapter 2:

$$u_t = -u - w * g(u)(u - u_R) + f \quad \text{and} \quad u(\cdot, 0) = u_0$$

(See the Section 2.5). We assume that the functions  $u$  and  $g$  are smooth (typically,  $g$  is a smooth approximation to the Heaviside function) and  $f$  has a bounded

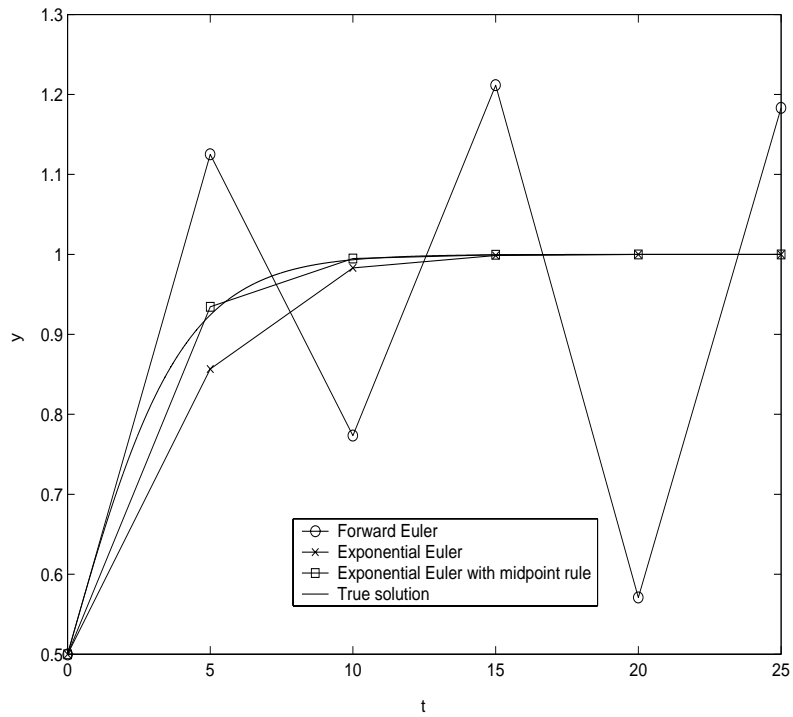


Figure 3.1: Logistic Equation on  $0 \leq t \leq 25$ . The true solution as well as the standard exponential Euler, Runge Kutta midpoint rule modification ((3.2) and (3.3)), and forward Euler approximation are plotted with  $h = 5$ .

derivative. Also, we assume that

$$|w(z)| \leq \rho(z) \text{ and } \int_{\mathbb{R}} \rho(z) dz = 1. \quad (3.18)$$

For simplicity, we assume that the function  $u$  is a scalar here. We do not consider existence. We could define  $u$  a priori and then determine  $f$ ; thus we argue there are problems for which there is a solution.

**Theorem 3.5.1** *Under the assumptions above, there is at most one solution to (2.3).*

**Proof:** Assume that  $u$  and  $v$  are the solutions to (2.3). Then we have

$$\begin{aligned} u_t &= -u - w * g(u)(u - 1) + f \\ v_t &= -v - w * g(v)(v - 1) + f. \end{aligned}$$

Let  $Y = u - v$ . Then,

$$\begin{aligned} Y_t &= -Y - w * (g(u)u - g(v)v + g(u) - g(v)) \\ &= -Y - w * \{g(u)Y + g'(\xi)Yv + g'(\xi)Y\} \\ &= -Y - w * P(u, v)Y \end{aligned}$$

where

$$P(u, v) = g(u) + g'(\xi)v + g'(\xi).$$

Since  $u$ ,  $v$ ,  $g$ , and  $g'$  are bounded,

$$\| P \|_{\infty} \leq M_P. \quad (3.19)$$

Then we have,

$$Y_t + Y = - \int_{\mathbb{R}} w(x-y)P(u,v)(y)Y(y) dx.$$

That is

$$\frac{d}{dt}(e^t Y(x, t)) = -e^t \int_{\mathbb{R}} w(x-y)P(u,v)(y, t)Y(y, t) dx.$$

Then,

$$\begin{aligned} e^t Y(x, t) - Y(x, 0) &= - \int_0^t e^s (w * (PY))(x, s) ds \\ Y(t) &= - \int_0^t e^{-(t-s)} (w * (PY))(x, s) ds \end{aligned}$$

since  $Y(\cdot, 0) = 0$ . Because we have (3.18) and (3.19),

$$\begin{aligned} |Y(x, t)| &\leq \int_0^t \int_{\mathbb{R}} |w(x-y)| \| P \|_{\infty} |Y(y, \cdot)| dy ds \\ &\leq M_P \int_0^t \int_{\mathbb{R}} \rho dy \| Y(\cdot, s) \|_{L^{\infty}(\mathbb{R})} ds \\ &\leq M_P \int_0^t \| Y(\cdot, s) \|_{L^{\infty}(\mathbb{R})} ds. \end{aligned} \quad (3.20)$$

Let  $F(t) = \int_0^t \| Y(\cdot, s) \|_{L^{\infty}(\mathbb{R})} ds$ , then (3.20) becomes

$$F'(t) \leq M_P F(t)$$

with  $F(0) = 0$  and  $F(t) \geq 0$ . This is a Gronwall type inequality. Hence,

$$\frac{d}{dt}(e^{-M_P t} F(t)) \leq 0$$

or

$$e^{-M_P t} F(t) - F(0) \leq 0.$$

Then we have  $F(t) \leq 0$ . Since we have  $F(t) \geq 0$ , we can conclude  $F \equiv 0$ . Therefore,

$$\| Y(\cdot, t) \|_{L^\infty(\mathbb{R})} = 0$$

for all  $t$ . Hence, we can conclude  $u = v$ , which completes our proof. ■

In our approximation we consider the semi-discrete case only; we obtain numerical solutions which will be discrete in time by using the exponential Euler approximation.

In order to apply the exponential Euler scheme, we let  $A(u) = f + w * g(u)u_R$  and  $B(u) = 1 + w * g(u)$ . If we let  $u_n$  be the numerical solution using the exponential Euler method to (2.3) and  $u$  be the true solution to (2.3), then we have

$$u(\cdot, t_n) = e^{-\int_{I_n} B(u(\cdot, s)) ds} u(\cdot, t_{n-1}) + \int_{I_n} e^{-\int_\tau^{t_n} B(u(\cdot, s)) ds} A(u(\cdot, \tau)) d\tau$$

and

$$u_n = e^{-B(u_{n-1})h} u_{n-1} + \frac{A(u_{n-1})}{B(u_{n-1})} (1 - e^{-B(u_{n-1})h})$$

where  $h$ ,  $t_n$ , and  $I_n$  have the same definitions as in Section 2.2.

**Theorem 3.5.2** *Under the assumptions above, there exists a constant  $C > 0$  so*

$$\| u(\cdot, t_n) - u_n \|_{L^\infty(\mathbb{R})} \leq Ch.$$

**Proof:** Let  $\sigma_n$  be the local truncation error of the method (2.3) on  $I_n$  defined by inserting the true solution  $u$  into the numerical approximation. Then,

$$u(\cdot, t_n) = e^{-B(u(\cdot, t_{n-1}))h} u(\cdot, t_{n-1}) + \frac{A(u(\cdot, t_{n-1}))}{B(u(\cdot, t_{n-1}))} (1 - e^{-B(u(\cdot, t_{n-1}))h}) + \sigma_n.$$

Therefore,

$$\begin{aligned} \sigma_n &= e^{-\int_{I_n} B(u(\cdot, s)) ds} u(\cdot, t_{n-1}) + \int_{I_n} e^{-\int_{\tau}^{t_n} B(u(\cdot, s)) ds} A(u(\cdot, \tau)) d\tau \\ &\quad - (e^{-B(u(\cdot, t_{n-1}))h} u(\cdot, t_{n-1}) + \frac{A(u(\cdot, t_{n-1}))}{B(u(\cdot, t_{n-1}))} (1 - e^{-B(u(\cdot, t_{n-1}))h})) \\ &= (e^{-\int_{I_n} B(u(\cdot, s)) ds} - e^{-B(u(\cdot, t_{n-1}))h}) u(\cdot, t_{n-1}) \\ &\quad + \int_{I_n} \{e^{-\int_{\tau}^{t_n} B(u(\cdot, s)) ds} A(u(\cdot, \tau)) \\ &\quad - e^{-\int_{\tau}^{t_n} B(u(\cdot, t_{n-1})) ds} A(u(\cdot, t_{n-1}))\} d\tau \tag{3.21} \\ &= P + Q. \end{aligned}$$

Then,

$$\begin{aligned} P &= e^{-\xi} \int_{I_n} (B(u(\cdot, s)) - B(u(\cdot, t_{n-1}))) ds \cdot u(\cdot, t_{n-1}) \\ &= e^{-\xi} u(\cdot, t_{n-1}) \int_{I_n} w * \{g(u(\cdot, t_{n-1})) - g(u(\cdot, s))\} ds \\ &= e^{-\xi} u(\cdot, t_{n-1}) \int_{I_n} w * \{g'(\eta_{n-1}) u_t(\cdot, \zeta_{n-1})(s - t_{n-1})\} ds. \end{aligned}$$

We used the mean value theorem on the first step with  $\xi$  in between  $B(u(\cdot, t_{n-1}))h$  and  $\int_{t_{n-1}}^{t_n} B(u) ds$  and on the third step with  $\zeta_{n-1}$  in between  $s$  and  $t_{n-1}$  and  $\eta_{n-1}$  in between  $u(\cdot, t_{n-1})$  and  $u(\cdot, s)$ . Since  $\xi$  and  $u(\cdot, t_{n-1})$  are bounded,  $|e^{-\xi} \cdot u(\cdot, t_{n-1})| \leq$

$C_0$  for some constant  $C_0$ ,

$$|P| \leq C_0 h \max_{x,n} |w * g'(\eta_{n-1})u_t(\cdot, \zeta_{n-1})h| = Ch^2.$$

Here, we used the assumptions that the functions  $g$  and  $u$  are smooth and bounded as well as assumption (3.18) to show

$$\max_{x,n} |w * g'(\eta_{n-1})u'(\zeta_{n-1})| \leq M \quad (3.22)$$

for some constant  $M$ . Now turning to the second term on the right side of (3.21), we have

$$\begin{aligned} Q &= \int_{I_n} \{e^{-\int_{\tau}^{t_n} B(u(\cdot, t_{n-1})) ds} (A(u(\cdot, t_{n-1})) - A(u(\cdot, \tau))) \\ &\quad + (e^{-\int_{\tau}^{t_n} B(u(\cdot, t_{n-1})) ds} - e^{-\int_{\tau}^{t_n} B(u(\cdot, s)) ds}) A(u(\cdot, \tau))\} d\tau. \end{aligned}$$

Substituting  $A(u) = f + w * g(u)u_R$  in the first term, we obtain

$$\begin{aligned} Q &= \int_{I_n} e^{-\int_{\tau}^{t_n} B(u(\cdot, t_{n-1})) ds} \left[ \frac{\partial f}{\partial t}(\psi_{n-1})(t_{n-1} - \tau) \right. \\ &\quad \left. + w * \{g'(\eta_{n-1})u_t(\cdot, \zeta_{n-1})(\tau - t_{n-1})\}u_R \right] d\tau \\ &\quad + \int_{I_n} \{e^{-\xi} \int_{\tau}^{t_n} w * \{g'(\nu_{n-1})u_t(\cdot, \phi_{n-1})(s - t_{n-1})\} ds A(u(\cdot, \tau))\} d\tau; \end{aligned}$$

We used the same analysis as for  $P$  for the second term in  $Q$ , above. We used the mean value theorem repeatedly on the second step. Then, using (3.22) and the fact that the functions  $\frac{\partial f}{\partial t}$  and  $u$  are bounded, we arrive at

$$|Q| \leq Ch^2$$

for some constant  $C$ . Therefore,  $|\sigma_n| = O(h^2)$ .

To show the global error estimate of the scheme for (2.3), we let  $F^n = u(\cdot, t_n) - u_n$ . Then,

$$\begin{aligned} F^n &= e^{-B(u(\cdot, t_{n-1}))h} u(\cdot, t_{n-1}) + \int_{I_n} e^{-\int_{\tau}^{t_n} B(u(\cdot, s)) ds} A(u(\cdot, t_{n-1})) d\tau \\ &\quad - (e^{-\int_{I_n} B(u_{n-1}) ds} u_{n-1} + \int_{I_n} e^{-\int_{\tau}^{t_n} B(u_{n-1}) ds} A(u_{n-1}) d\tau) + \sigma_n \\ &= G + H + \sigma_n \end{aligned}$$

where  $G$  consists of the first and the third terms and  $H$  is the second and the fourth terms. If we add and subtract  $e^{-\int_{I_n} B(u_{n-1}) ds} u(\cdot, t_{n-1})$  to  $G$ , then

$$\begin{aligned} |G| &= |\{e^{-\int_{I_n} B(u(\cdot, t_{n-1})) ds} - e^{-\int_{I_n} B(u_{n-1}) ds}\} u(\cdot, t_{n-1}) \\ &\quad + e^{-\int_{I_n} B(u_{n-1}) ds} (u(\cdot, t_{n-1}) - u_{n-1})| \\ &\leq e^{-\xi} \int_{I_n} |w * (g(u(\cdot, t_{n-1})) - g(u_{n-1}))| ds \cdot |u(\cdot, t_{n-1})| \\ &\quad + |e^{-\int_{I_n} B(u_{n-1}) ds}| \cdot |F^{n-1}|. \end{aligned}$$

The exponents in both of the exponential functions above are  $O(h)$  so there exists a constant  $K$  so

$$\begin{aligned} |G| &\leq (1 + Kh) \left\{ \int_{I_n} |w * g'(\eta_{n-1}) F^{n-1}| ds |u(\cdot, t_{n-1})| + |F^{n-1}| \right\} \\ &\leq (1 + Kh) (h \cdot |w * g'(\eta_{n-1}) F^{n-1}| |u(\cdot, t_{n-1})| + |F^{n-1}|) \\ &\leq (1 + Kh) \|F^{n-1}\|_{L^\infty(\mathbb{R})} \end{aligned}$$

where  $\|\cdot\|_{L^\infty(\mathbb{R})}$  is the  $L^\infty$ -norm over the real line in the  $x$ -variable.

Next, if we add and subtract  $\int_{I_n} e^{-\int_{\tau}^{t_n} B(u_{n-1}) ds} A(u(\cdot, t_{n-1})) d\tau$  to  $H$ , then

$$\begin{aligned}
|H| &= \left| \int_{I_n} \left[ e^{-\int_{\tau}^{t_n} B(u(\cdot, s)) ds} - e^{-\int_{\tau}^{t_n} B(u_{n-1}) ds} \right] A(u(\cdot, t_{n-1})) \right. \\
&\quad \left. + e^{-\int_{\tau}^{t_n} B(u_{n-1}) ds} \{A(u(\cdot, t_{n-1})) - A(u_{n-1})\} d\tau \right| \\
&\leq \int_{I_n} \left[ |e^{\xi}| \int_{\tau}^{t_n} |B(u_{n-1}) - B(u(\cdot, t_{n-1}))| ds |A(u(\cdot, t_{n-1}))| \right. \\
&\quad \left. + e^{\int_{\tau}^{t_n} B(u_{n-1}) ds} \left\{ \left| \frac{\partial f}{\partial t}(\psi_{n-1})(t_{n-1} - \tau) + u_R \cdot w * (g(u(\cdot, t_{n-1})) - g(u_{n-1})) \right| \right\} d\tau \right] \\
&\leq Ch \|F^{n-1}\|_{L^\infty(\mathbb{R})} + O(h^2).
\end{aligned}$$

So,

$$\begin{aligned}
|F^n| &\leq |G| + |H| \\
&\leq (1 + Kh) \|F^{n-1}\|_{L^\infty(\mathbb{R})} + O(h^2)
\end{aligned}$$

or

$$\|F^n\|_{L^\infty(\mathbb{R})} \leq (1 + Kh)^n + Lh^2 \{1 + (1 + Kh) + \dots + (1 + Kh)^{n-1}\} \|F^0\|_{L^\infty(\mathbb{R})}$$

for some constant  $L$ . Now, by the standard iteration argument (see [A]),

$$\|F^n\|_{L^\infty(\mathbb{R})} \leq C (\|F^0\|_{L^\infty(\mathbb{R})} + h).$$

Therefore, we can conclude that the exponential Euler method applied to the above integro-differential equation is first order accurate (i.e. the global error is  $O(h)$ ). ■

Numerical results of the scheme applied to an integro-differential equation are presented in Section 3.7.

### 3.6 Applications to Partial Differential Equations

In this section we suggest a way to use splitting methods to extend the range of application of the exponential Euler scheme to certain partial differential and integro-differential equation models of neuron activity where a diffusion operator is involved.

The Hodgkin-Huxley model for electrical activity along an axon is described by a reaction-diffusion equation for the membrane potential. After nondimensionalization, it has the following form

$$\frac{\partial v}{\partial t} = D \frac{\partial^2 v}{\partial x^2} + f(v, m, n, h, \dots). \quad (3.23)$$

There are also channel equations for  $m, n, h, \dots$  which would have the same form as equation (2.1).

When applying exponential Euler to a typical reaction-diffusion equation, one is confronted with the choice of whether to place the diffusion in the  $A(y)$  or  $B(y)y$  terms. Inclusion of the diffusion in the  $A(y)$  term leads to an explicit treatment of the diffusion and therefore a time step restriction is required. Inclusion in the  $B(y)y$  term leads to the evaluation of a matrix exponential (of the diffusion operator). Both of these approaches would typically be considered too expensive computationally. We therefore, suggest the use of a splitting scheme.

To apply the splitting method to (3.23), we introduce the following equations:

$$\frac{\partial z}{\partial t} = D \frac{\partial^2 z}{\partial x^2} \quad \text{and} \quad z(\cdot, 0) = z_0 \quad (3.24)$$

and

$$\frac{\partial u}{\partial t} = f(u, m, n, h, \dots) \quad \text{and} \quad u(\cdot, 0) = u_0. \quad (3.25)$$

Let  $z(\cdot, t) = X^t z_0$  and  $u(\cdot, t) = Y^t u_0$  be the solutions of (3.24) and (3.25) respectively. These two formulas are combined over a time step interval of length  $\Delta t$  to produce a splitting method approximation. If  $v_{n-1}$  is an approximation to  $v(\cdot, t_{n-1})$  then the splitting method solution at time  $t_n$  would be

$$v_n = X^{\Delta t} Y^{\Delta t} v_{n-1}.$$

The Strang formula typically would provide more accuracy and be defined by

$$v_n = X^{\Delta t/2} Y^{\Delta t} X^{\Delta t/2} v_{n-1}$$

([BBD] and [Sb]). The equation (3.25) is a standard linear diffusion equation that can be solved efficiently by many time discretization methods. We suggest that the exponential Euler scheme could be used to approximate  $Y^t$ . Here, the  $f$  term will typically have the same form as in (3.1).

### 3.7 Numerical Results

In this section, we present some computational results with the exponential Euler scheme applied to the logistic equation, the FitzHugh-Nagumo equation and an integro-differential equation similar to (2.3). For comparison in the ODE cases we also experimented with the forward Euler method as well as the midpoint extension of the exponential Euler scheme introduced in Section 3.2.

We have also created and numerically tested another extension of the exponential Euler scheme using a multistep idea. We used

$$\tilde{y}_n = \frac{3}{2}y_n - \frac{1}{2}y_{n-1} \tag{3.26}$$

in the form (3.2) and the method computationally showed the second order accuracy (See figure 3.2).

First, we present our numerical results for the logistic equation (3.15)

$$y' = \beta y(1 - y), \quad \text{with } y(0) = y_0 \quad \text{where } \beta > 0 \text{ and real.}$$

with  $\beta = 0.5$  and initial condition  $y(0) = 0.5$  (Figure 3.1). The true solution of the logistic equation is  $y(t) = y_0((1 - y_0)e^{-\beta t} + y_0)^{-1}$ .

Figure 3.2 shows the error vs  $h$  plots for forward Euler, exponential Euler, as well as the midpoint and multistep extensions. The slope of the lines is the experimental order of convergence for each of the methods. Careful study of the graphs reveals

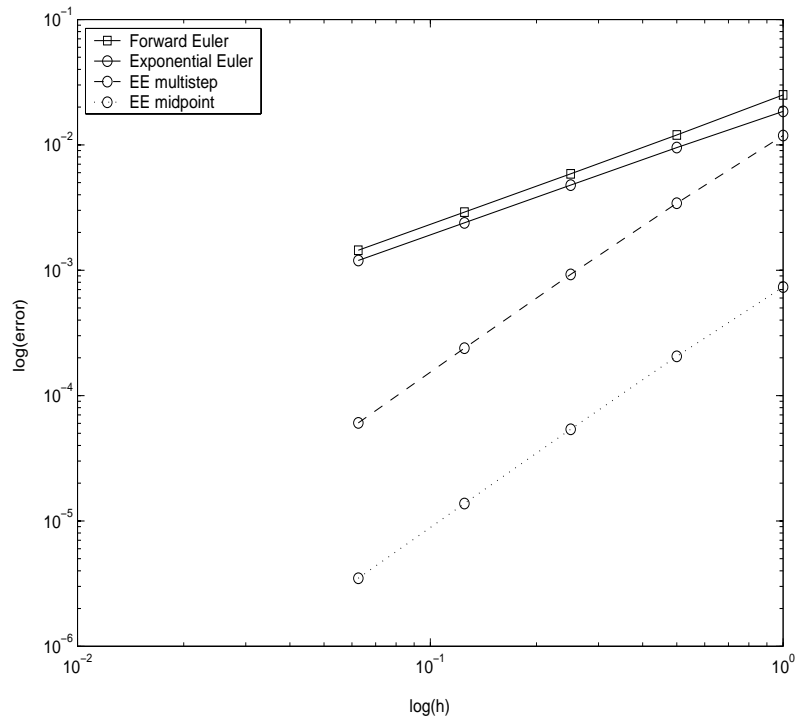


Figure 3.2: Error of the each methods: forward Euler, standard exponential Euler, Runge-Kutta midpoint rule modification (3.2 and 3.3), and the multistep extension (3.2 and 3.26). Logarithmic scales are used for both the x- and y- axes.

the midpoint and multistep methods are second order while the two Euler methods are first order.

As a second example, we present the Fitzhugh-Nagumo equation (2.2) which was introduced in Section 2.3. Here we have

$$\begin{aligned} f(v, w) &= v(v - 0.1)(1 - v) - w \\ \text{and } g(v, w) &= v - 0.5w \end{aligned} \tag{3.27}$$

and  $0 \ll \epsilon \ll 1$ .

We have carried out numerical experiments with the different applied currents  $I = 0.0$ , and  $I = 0.5$ . Figure 2.4 is a plot of the solutions of the FitzHugh-Nagumo equations with  $I = 0.0$  and  $I = 0.5$ . Here we used the forward Euler method with the stepsize  $h = 10^{-6}$  as a solution of the FitzHugh-Nagumo equation to calculate the error of the schemes. Our results are in Tables 3.1 and 3.2. Here, FE, EE, EEMP, and EEMS are the acronyms of forward Euler, exponential Euler, exponential Euler with midpoint rule, and exponential Euler with multistep method, respectively. These tables demonstrate that the forward Euler method is unstable for large  $h$  while the exponential Euler methods are not. We also observe from the table that the forward and exponential Euler methods are  $O(h)$  since their errors are divided by  $1/2$  on each reduction of stepsize. At the same time the results suggest that the exponential Euler extensions are  $O(h^2)$ .

Finally, we have tested the scheme on one example of the integro-differential

h	FE	EE	EEMP	EEMS
.05	$\infty$	1.1346	0.8258	0.8935
.025	0.5223	0.1294	0.0532	0.1351
.010	0.2493	0.0476	0.0042	0.0078
.0050	0.1358	0.0228	0.0009	0.0017
.0025	0.0688	0.0115	0.0002	0.0004

Table 3.1: Errors in approximation of solutions to FitzHugh-Nagumo equation with  $I = 0.0$  and  $0 \leq t \leq 1$ .

h	FE	EE	EEMP	EEMS
.025	$\infty$	1.2035	0.6373	1.3049
.010	0.8691	0.5616	0.0763	0.7271
.005	0.6072	0.3143	0.0136	0.0297
.0025	0.3580	0.1634	0.0026	0.0071
0.00125	0.1889	0.0823	0.0006	0.0018

Table 3.2: Errors in approximation of solutions to FitzHugh-Nagumo equation with  $I=0.5$  and  $0 \leq t \leq 5$ .

equation. Consider the following integro-differential equation

$$u_t = -u - w * H(u - \theta)(u - 1) \quad (3.28)$$

where  $H$  is the Heaviside function

$$H(s) = \begin{cases} 1 & \text{for } s > 0 \\ 0 & \text{otherwise} \end{cases}$$

and

$$w * H(u - \theta) = \int_{-\infty}^{\infty} w(\cdot - y)H(u(y, t) - \theta) dy$$

is similar to the one we analyzed above. However, because of the jump discontinuity in  $H$  our Theorem 3.5.2 does not apply. Nevertheless, it is interesting to see if the  $O(h)$  convergence still holds.

In order to calculate the true solution of the (3.28), we have studied traveling front solutions to (3.28) that are introduced by ([PE]). We let the traveling front solution  $U$  to (3.28) be monotone decreasing with  $U(-\infty) = A$ ,  $U(\infty) = 0$ ,  $U(0) = \theta$  and  $c$  of constant value ([PE]). And we substitute  $u(x, t) = U(x - ct)$  in (3.28) and let  $z = x - ct$ . Then we have,

$$cU'(z) = U(z) + (w * H(U - \theta))(U(z) - 1). \quad (3.29)$$

And

$$(w * H(U(z) - \theta))(z) = \int_{-\infty}^{\infty} w(z - \zeta)H(U(\zeta) - \theta) d\zeta$$

where  $\zeta = y - ct$ . Then

$$\begin{aligned} (w * H(U(z) - \theta))(z) &= \int_{-\infty}^0 w(z - \zeta) d\zeta \\ &:= W(z). \end{aligned}$$

Let

$$G(z) := \int_0^z \frac{1}{c} (1 + W(\zeta)) d\zeta,$$

then the solution to (3.29) is

$$U(z) = \theta e^{G(z)} - \frac{1}{c} e^{G(z)} \int_0^z e^{-G(\zeta)} W(\zeta) d\zeta$$

where

$$\theta = \frac{1}{c} \int_0^\infty e^{-G(\zeta)} W(\zeta) d\zeta$$

.

To apply the exponential Euler scheme to (3.28), we let

$$A(u) = w * H(u - \theta)$$

and

$$B(u) = 1 + w * H(u - \theta).$$

We used  $w(x) = \frac{1}{2}$  when  $-1 \leq x \leq 1$  and  $w(x) = 0$  otherwise in our computation.

Here we are computing a fully discrete approximation on a spatial mesh with subinterval width  $\Delta x$ . We used the rectangular rule with mesh parameter width  $10^{-6}$

	h=0.05	h=0.1	h=0.2	h=0.4
$\Delta x=.01$	0.00742	0.01277	0.02306	0.04094
$\Delta x=.02$	0.00880	0.01441	0.02483	0.04168
$\Delta x=.04$	0.00517	0.00858	0.01553	0.03272

Table 3.3: Errors in approximation of solutions to the integro-differential Equation with  $-.5 \leq x \leq .5$ , and  $0 \leq t \leq 10$

to evaluate the convolutions in the true solution. Table 3.3 verifies that our fully discrete exponential Euler method is nearly first order accurate ( $O(h)$ ). Of course, our Theorem 3.5.2 only applies to semi-discrete methods with smooth  $g$ .

## Chapter 4

# Mathematical Model of Retinal Waves in Visual Cortex

In this Chapter, we present a one-dimensional firing rate type model for retinal waves that produces similar results to those in ([BFSR] and [FBARS]). In the developing mammalian retina, spontaneous neuronal activity, called retinal waves, can be detected and it is known that a synaptically connected network of amacrine cells and ganglion cells in the retina is involved in generating these waves ([WCSS], [FWSWS]). Feller et al ([FBARS]) has created a two layer readout model that consists of those two cell types. In their model, ganglion cells receive excitatory inputs and depolarize through synaptic coupling only if nearby amacrine cells reach their threshold. The ganglion cells cannot cause nearby ganglion cells or amacrine

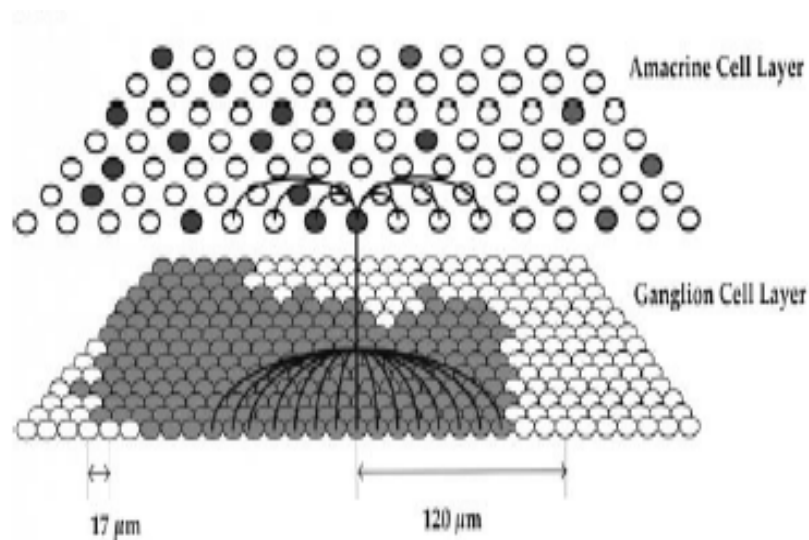


Figure 4.1: Schematic of Retinal Model (Page 3582 of [BFSR])

cells to depolarize (See Figure 4.1). Because of this we focus on the amacrine cells only.

The primary goal in this chapter is the introduction of the firing-rate model of amacrine cells in the retina and confirmation through computer simulation of their validity. In particular, they should match the following three experimentally testable quantities:

- The wave velocities should be in the range of 0.2-0.6 mm/sec (see page 3580 of [BFSR]).
- The average length covered by an individual wave should be approximately

0.55 mm (This the square root of 0.298 mm<sup>2</sup> which is noted as the average area on page 3583-3584 of [BFSR]).

- The average interval in time between waves should be around 126 seconds (see page 3583-3584 of [BFSR]).

Our model network consists of a one-dimensional array of  $N$  neurons which represent the amacrine cell layer. As in [FBARS] the cells are assumed to be 34  $\mu\text{m}$  apart and  $N \cong 70$ ; thus the array has length around 2 mm.

## 4.1 Model Description

Our model for the amacrine cell layer is based on firing rate techniques that includes a slow calcium variable. The main equation for an individual amacrine cell  $n$  contains five different currents as follows:

$$C \frac{d\tilde{v}_n}{dt} = I_{Ca} + I_{AHP} + I_{Rest} + I_{Syn} + I_{Noise} \quad (4.1)$$

$$\frac{d\tilde{c}_n}{dt} = -fI_{Ca} - \frac{\tilde{c}_n}{\tau_c} \quad (4.2)$$

where

$$I_{AHP} = -g_{AHP} \frac{\tilde{c}_n}{K_c} (\tilde{v}_n - v_{Rest}),$$

$$\begin{aligned}
I_{Syn} &= -g_{Syn} \sum_{\ell \in F_n} \tilde{w}_{\ell,n} H(\tilde{v}_\ell - \tilde{\theta})(\tilde{v}_n - v_{Ca}) \\
I_{Rest} &= -g_L(\tilde{v}_n - v_{Rest}), \\
I_{Ca} &= -g_{Ca} H(\tilde{v}_n - \tilde{\theta})(\tilde{v}_n - v_{Ca}),
\end{aligned}$$

for  $n = 1, 2, \dots, N$  and

$$H(s) = \begin{cases} 1 & \text{for } s > 0 \\ 0 & \text{otherwise} \end{cases}$$

is the Heaviside function. Here  $\tilde{v}_n(\tilde{t})$  and  $\tilde{c}_n(\tilde{t})$  represent the membrane potential and cytoplasmic calcium concentrations of amacrine cell  $n$ . The set  $F_n$  has the indices of the amacrine cells connected to cell  $n$ . We connected each amacrine cell to its 6 neighbors; 3 on each side.

The first current  $I_{Ca}$  is a spiking current which corresponds to the rapid depolarization of the amacrine cell. If a cell reaches its threshold ( $\tilde{\theta}$ ),  $I_{Ca}$  is turned on due to the Heaviside function  $H$  causing the cell to be depolarized. There is a current due to the  $Ca^{2+}$  activated  $K^+$  channels ( $I_{AHP}$ ). This after-hyperpolarizing current is thought to be important for termination of action potentials and determination of the refractory period ([T] and [SG]). The depolarization of a cell causes an increase in the intracellular calcium concentration level, so that the  $I_{AHP}$  current dominates and the cell returns to resting potential. After a cell fires an action potential, it enters its refractory period. The amacrine cell in our model has a long refractory period because of the slow calcium variable and the time constant  $\tau_c$ .

The third current  $I_{Rest}$  is a leak current. Nonrefractory amacrine cells can reach their thresholds either through excitatory inputs from neighboring cells (synaptic currents) or through an intrinsic spontaneous depolarization (noise currents). In our model, there is a synaptic current  $I_{Syn}$  which corresponds to inputs from nearby amacrine cells. Finally, there is a noise current  $I_{Noise}$  which represents the current from spontaneous random noise events that the cells experience and instigates the waves. Here,

$$I_{Noise}(t) = \sum_j \tilde{M}_{Noise} P(\tilde{t} - \tilde{t}_j^{Noise}, \tilde{\tau}_{Noise})$$

where  $P(s, \gamma)$  is a unit pulse function that lasts for  $\gamma$  time units after  $s = 0$ ;

$$P(s, \gamma) = \begin{cases} 1 & \text{if } s \in [0, \gamma] \\ 0 & \text{otherwise.} \end{cases}$$

Thus  $\tilde{\tau}_{Noise}$  is the length of each spontaneous noise event and  $\tilde{M}_{Noise}$  is the magnitude. The  $\tilde{t}_j^{Noise}$  are the times of the noise events for each individual neuron. These times occur at random intervals of length, on average,  $\tilde{N}_{Noise}$ , with standard deviation  $\tilde{N}_{Noise}/2$ . We have chosen  $\tilde{N}_{Noise}$  as the value used in [FBARS].

We now nondimensionalize the equations describing the amacrine cells. We make the following variable changes; our primary goal is to match the nondimensionalized model with the automata-type model used in [FBARS]. We introduced the extra nondimensional parameters  $\rho_L$  and  $\theta$  to accomplish this.

$$\tilde{v}_n = v_{Rest} + \frac{\tilde{\theta} - v_{Rest}}{\phi} v_n, \quad \tilde{c}_n = K_c c_n \quad \text{and} \quad \tilde{t} = \frac{C \rho_L}{g_L} t.$$

Thus we have a characteristic time  $t_c = C\rho_L/g_L$ . We also set

$$i_{Noise} = \sum_j M_{Noise} P(\cdot - t_j^{Noise}; \tau_{Noise}).$$

After the variable changes we have the following nondimensional system

$$v'_n = -\rho_L v_n - \rho_{Ca} H(v_n - \phi)(v_n - \theta) - \rho_{AHP} c_n v_n - (v_n - \theta) \sum_{\ell \in F_n} w_{\ell,n} H(v_\ell - \phi) + i_{Noise}$$

and

$$c'_n = \alpha H(v_n - \phi)(v_n - \theta) - \frac{c_n}{\tau}.$$

where we introduce the following nondimensional parameters:

$$\begin{aligned} \rho_{Ca} &= g_{Ca}\rho_L/g_L, \quad \rho_{AHP} = g_{AHP}\rho_L/g_L, \quad \alpha = \frac{f g_{Ca}\rho_L C(\tilde{\theta} - v_{Rest})}{g_L K_c \phi}, \\ \tau &= \tau_c/t_c, \quad \tau_{Noise} = \tilde{\tau}_{Noise}/t_c, \quad \theta = \phi \frac{v_{ca} - v_{Rest}}{\tilde{\theta} - v_{Rest}}, \\ M_{Noise} &= \frac{\rho_L \phi}{g_L(\tilde{\theta} - v_{Rest})} \tilde{M}_{Noise} \quad \text{and} \quad w_{\ell,n} = \rho_L \tilde{w}_{\ell,n}. \end{aligned}$$

Choosing  $\rho_L = 1$  and  $\phi = 1$  we have, using the constants from table 1,

$$\rho_{Ca} = 1, \quad \rho_{AHP} = 1.5, \quad w_{\ell,n} = .5, \quad t_c = 25 \text{ ms}, \quad \theta = 3, \quad \hat{\alpha} = .5 \quad \text{and} \quad \tau = 800.$$

This completes the description of our nondimensionalize model of the amacrine cells.

Membrane Potentials	$v_{Ca} = 80 \text{ mV}$	$v_{Rest} = -70 \text{ mV}$
Threshold Potentials	$\tilde{\theta} = -20 \text{ mV}$	
Capacitance	$C = 1 \mu \text{ F/cm}^2$	
Conductances	$g_L = 0.04 \text{ mS/cm}^2$	$g_{AHP} = 0.06 \text{ mS/cm}^2$
	$g_{Ca} = 0.04 \text{ mS/cm}^2$	
Calcium Parameters	$K_c = 1 \mu \text{M}$	$\tau_c = 20 \text{ s}$
	$f = 1 \times 10^{-2} \mu \text{M cm}^2 / (\mu \text{A ms})$	
Synaptic Current	$g_{Syn} = 2 \text{ mS/cm}^2$	$\tilde{w}_{\ell,n} = 1/2$
Noise Current	$\tilde{M}_{Noise} = 6 \mu \text{A}$	$\tilde{\tau}_{Noise} = 1 \text{ s}$
	$\tilde{N}_{Noise} = 28 \text{ s}$	

Table 4.1: Physical Parameters used in this Study

## 4.2 Computational Results

In this section, we present the computational results of the firing rate model of amacrine cells. As mentioned in the previous section, we have introduced three testable quantities : the wave velocities, the average length covered by an individual wave and the average interval in time between waves. With the nondimensionalized model of amacrine cells, we have compared these quantities from the computational results to those in [BFSR] and [FBARS].

There are 70 amacrine cells in our model and the cells are assumed to be  $34 \mu m$  apart from each other. We have solved the differential equations of the model with the exponential Euler scheme and  $h(= \Delta t) = .05$ .

Figure 4.2 shows that the waves created in our one dimensional amacrine cell model. We have calculated the average wave speed with 7 randomly chosen waves and found it was around 3.0451 mm/sec which though large is still within the range of order of magnitude for the wave speed (0.2 - 0.6 mm/sec) in [BFSR]. Figure 4.3 shows a single wave on a short time scale; the shape of the line provides a rough approximation of the wave speed. In this example, the speed is  $3.67 mm/s$ .

Also we examined the average length covered by an individual wave with 25 randomly chosen waves. The average length of waves are approximately .4 mm which is also within the range of order of magnitude for the average length covered

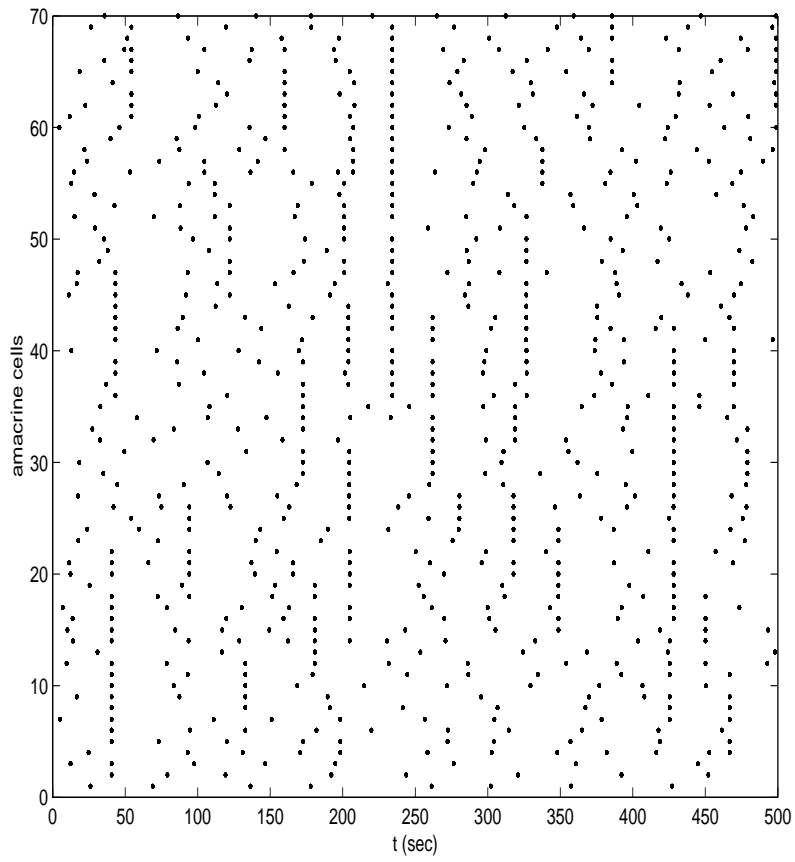


Figure 4.2: Waves (dots in vertical lines) are created.

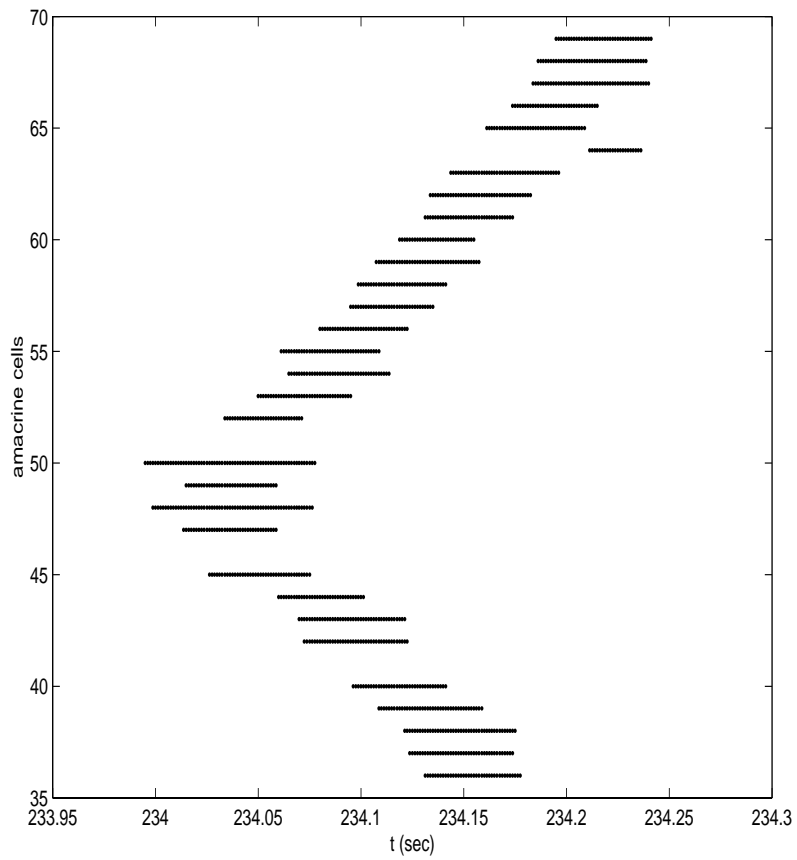


Figure 4.3: A wave in figure 4.2 is zoomed in.

by an individual wave. The average interval in time between waves were about 90 seconds that is also within the range of order of magnitude for the refractory periods.

### 4.3 Integro-Differential Equation Modeling

A synaptically coupled network of neurons is often described by an integro-differential equation (IDE). Our amacrine cell model can also be transformed into an integro-differential problem. We follow the approach in [TEY] to transform the network into an IDE problem. We simplify by assuming the neurons lie on the entire real axis and neuron  $n$  is placed at position  $x_n = n\Delta x$  where, for amacrine cells, we take  $\Delta x = 34\mu\text{m}$  and  $n = 0, \pm 1, \pm 2, \dots$ . We define

$$w(s) = \begin{cases} .5 & \text{for } |s| < 120\mu\text{m} \\ 0 & \text{otherwise} \end{cases}$$

as a continuum representation for  $w_{\ell,n}$ . Recall  $w_{\ell,n} = 0.5$  and each cell was connected synaptically to its six nearest neighbors; so its range was around  $120\mu\text{m}$  in each direction. Our IDE model will have continuum functions  $v, c$ , and  $i$  so

$$v(x_n, t) \cong v_n(t), \quad c(x_n, t) \cong c_n(t), \quad \text{and} \quad i(x_n, t) \cong i_{Noise}(t; n).$$

So, for the membrane potential equation for the amacrine cells we have, at say,  $x_n$  and  $t$ ,

$$\frac{\partial v}{\partial t} = -\rho_L v + \rho_{Ca} H(v - \phi)(v - \theta) - \rho_{AHPC} v - \frac{1}{\Delta x} (v - \theta) \sum_{\ell} w(\cdot - x_{\ell}) H(v(x_{\ell}, \cdot) - \phi) \Delta x + i$$

Taking  $x$  in place of  $x_n$ ,  $y$  in place of  $x_{\ell}$ , and approximating the synaptic current sum by an integral over  $y$  we have, for any  $x$ ,

$$\frac{\partial v}{\partial t} = -\rho_L v + \rho_{Ca} H(v - \phi)(v - \theta) - \rho_{AHPC} v + \frac{1}{\Delta x} (v - \theta) \int_{\mathbf{R}} w(\cdot - y) H(v(y, \cdot) - \phi) dy + i.$$

Similarly, we have

$$\frac{\partial c}{\partial t} = \alpha H(v - \phi)(v - \theta) - \frac{c}{\tau}.$$

We expect standard mathematical techniques (similar to those in [Cs], [GE], [PE], or [TEY]) could be used to derive traveling wave solutions of this IDE model, speeds and pulse shapes.

## 4.4 Future Work

There are several improvements and extensions that should be made to our retinal wave model. First of all, the model should contain a ganglion cell layer as the cellular automata model in [FBARS] and [BFSR]. Since the retinal waves are observed in

ganglion cell layer, it is important to include this cell type in the model even though our model already reproduces the spatiotemporal patterns of retinal waves. To compare our model to experimental data more precisely, we should introduce two-dimensional geometry.

Our wave speeds were slightly large; to remodeling this we could introduce a more complex synaptic response that allows a finite rise time instead of the Heaviside function response we currently have.

Of course, the primary extension would involve an analysis of the IDE model introduced in Section 4.3. For instance, one should be able to find traveling waves and deduce their speed as is done in, say, ([TEY]).

# Bibliography

- [A] K. Atkinson, *An Introduction to Numerical Analysis*, John Wiley & Sons, (1988).
- [AL] R. Anguelov and J. Lubuma, Contributions to the mathematics of the non-standard finite difference method and applications, *Numer. Math. Part. Diff. Equ.*, **17** (2001), 518-543.
- [BB] J.M. Bower and D. Beeman, *The Book of GENESIS*, Springer-Verlag, (1998).
- [BBD] C. Besse, B. Bidégaray, and S. Descombes, Order Estimates in Time of Splitting Methods for the Nonlinear Schrödinger Equation, *SIAM J. Numer. Anal.*, **40**, 26-40.
- [BFSR] D.A. Butts, M.B. Feller, C.J. Schatz, and D.S. Rokhsar, Retinal waves are governed by collective network properties, *J. Neurosci.*, **19** (1999), 3580-3593.

- [C] D.R. Copenhagen, Retinal development: on the crest of an exciting wave, *Curr. Biol.*, **6** (1996), 1368-1370.
- [Cs] S. Coombs, Dynamic of synaptically coupled integrate-and-fire-or-burst neurons (Preprint).
- [D] S. Descombes, Convergence of a Splitting Method of High Order for Reaction-Diffusion Systems, *Math. Comp.*, **70**, 1481-1501.
- [F] C.P. Fall, E.S. Marland, J.M. Wagner, and J.J. Tyson, *Computational Cell Biology*, Springer, (2002).
- [FBARS] M.B. Feller, D.A. Butts, H.L. Aaron, D.S. Rokhsar, and C.J. Shatz, Dynamic processes shape spatiotemporal properties of retinal waves, *Neuron*, **19** (1997), 293-306.
- [FWSWS] M.B. Feller, D.P. Wellis, D. Stellwagen, F.S. Werblin, and C.J. Shatz, Requirement for cholinergic synaptic transmission in the propagation of spontaneous retinal waves, *Science*, **272** (1996), 1182-1187.
- [GE] D. Golomb, Models of neuronal transient synchrony during propagation of activity through neocortical circuitry, *J. Neurophysiol.*, **79** (1998), 1-12.

- [HK] A.L. Hodgkin, A.F. Huxley, and B. Katz, Measurement of current-voltage relations in the membrane of the giant axon of *Loligo*, *J. Physiol.*, **116** (1952), 424-448.
- [HHa] A.L. Hodgkin, A.F. Huxley, and B.Katz, Measurement of current-voltage relations in the membrane of the giant axon of *Loligo*, *J. Physiol.*, **116** (1952), 424-448.
- [HHb] A.L. Hodgkin and A.F. Huxley, Currents carried by sodium and potassium ions through the membrane of the giant axon of *Loligo*, *J. Physiol.*, **116** (1952), 449-472.
- [HHc] A.L. Hodgkin and A.F. Huxley, The components of membrane conductance in the giant axon of *Loligo*, *J. Physiol.*, **116** (1952), 473-496.
- [HHd] A.L. Hodgkin and A.F. Huxley, The dual effect of membrane potential on sodium conductance in the giant axon of *Loligo*, *J. Physiol.*, **116** (1952), 497-506.
- [HH] A.L. Hodgkin and A.F. Huxley, A quantitative description of membrane current and its application to conduction and excitation in nerve, *J. Physiol.*, **117** (1952), 500-544.

- [I] A. Iserles, Stability and Dynamics of Numerical Methods for Nonlinear Ordinary Differential Equations, *IMA J. of Num. Anal.*, **10** (1990), 1-30.
- [KS] J. Keener and J. Sneyd, *Mathematical Physiology*, Springer, (1998).
- [LTGE] C.R. Laing, W.C. Troy, B.Gutkin, and G.B. Ermentrout, Multiple bumps in a neuronal model of working memory, *SIAM J. Appl. Math.*, **63** (2002), 62-97.
- [Ma] R.H. Masland, Maturation of function in the developing rabbit retina, *J. Comp. Neurol.*, **175** (1977), 275-286.
- [M1] R.E. Mickens, editor, *Application of nonstandard finite difference scheme*, World Scientific, Singapore, (2000).
- [M2] R.E. Mickens, A best finite difference method for the Fisher equation, *Num. Meth. Part. Diff. Eqs.*, **10** (1994), 581-585.
- [M3] R.E. Mickens, Relation between time and space step-sizes in nonstandard finite difference schemes for the Fisher equation, *Num. Meth. Part. Diff. Eqs.*, **13** (1997), 51-55.
- [MG] L. Maffei and L. Galli-Resta, Correlation in the discharges of neighboring rat retinal ganglion cells during prenatal life, *Proc. Natl. Acad. Sci. USA*, **87** (1990), 2861-2864.

- [ML] C. Morris and H. Lecar, Voltage oscillations in the barnacle giant muscle fiber, *Biophys. J.*, **35** (1981), 193-213.
- [MWBS] M. Meister, R.O. Wong, D.A. Baylor, and C.J. Shatz, Synchronized bursts of action potentials in ganglion cells of the developing mammalian retina, *Science*, **252** (1991), 939-943.
- [O] J. Oh, and D.A. French, Error Analysis of the Exponential Euler Method and Mathematical Modeling of the Retinal Waves in Neuroscience, *Appl. Math. Comput.*, in press.
- [PE] D.J. Pinto and G.B. Ermentrout, Spatially Structured Activity in Synaptically Coupled Neuronal Networks: 1. Traveling Fronts and Pulses, *SIAM J. Appl. Math.*, (2001) **62**, 206-225.
- [RG] J.I. Ramos and C.M. Garcia-Lopez, Piecewise-linearized methods for initial-value problems, *Appl. Math. Comp.*, **82** (1997), 273-302.
- [RU] Rizwan-Uddin, Comparison of the nodal integral method and nonstandard finite-difference schemes for the Fisher equation, *SIAM J. Sci. Stat. Comput.*, **22** (2001), 1926-1942.
- [Sa] Q. Sheng, Solving Linear Partial Differential Equations by Exponential Splitting, *IMA J. Numer. Anal.* **9** (1989), 199-212.

- [Sb] G. Strang, On the Construction and Comparison of Difference Schemes, *SIAM J. Numer. Anal.* **5**, (1968) 507-517.
- [SG] E. Sernagor and N.M. Grzywacz, Influence of spontaneous activity and visual experience on developing retinal receptive fields, *Curr. Biol.*, **6** (1996), 1503-1508.
- [SLT] J. Sundnes, G.T. Lines, and A. Tveito, Efficient Solution of Ordinary Differential Equations Modeling Electrical Activity in Cardiac Cells, *Math. Bioscience*, **172** (2001), 55-72.
- [T] D.H. Terman, Dynamics of Singularly Perturbed Neural Networks, *Proceedings of Symposia in Applied Mathematics*, (2000).
- [TEY] D.H. Terman, G.B. Ermentrout, and A.C. Yew, Propagating Activity Patterns in Thalamic Neuronal Networks, *SIAM J. Appl. Math.*, **61** (2001) 1578-1604.
- [WMS] R.O. Wong, M. Meister, and C.J. Shatz, Transient period of correlated bursting activity during development of the mammalian retina, *Neuron*, **11** (1993), 923-938.
- [WCSS] R.O. Wong, A. Chernjavsky, S.J. Smith, C.J. Shatz, Early functional neural networks in the developing retina, *Nature*, **374** (1995), 716-718.

- [Y] R. Yuste, Introduction: Spontaneous activity in the developing central nervous system, *Semin. Cell. Dev. Biol.*, **8** (1997), 1-4.
- [Z] M.J. Zigmond, F.E. Bloom, A.C. Landis, J.L. Roberts, and L.R. Squire, *Fundamental Neuroscience*, Academic Press, (1999).